Molecular Therapy
Original Article

# Lentiviral Vector-Based Dendritic Cell Vaccine Suppresses HIV Replication in Humanized Mice

Thomas D. Norton,[1,2,4] Anjie Zhen,[3,4] Takuya Tada,[1] Jennifer Kim,[3] Scott Kitchen,[3] and Nathaniel R. Landau[2]

[1]Department of Medicine, Division of Infectious Diseases, NYU Langone Medical Center, New York, NY 10016, USA; [2]Department of Microbiology, NYU Langone Medical Center, New York, NY 10016, USA; [3]Department of Medicine, Division of Hematology and Oncology, The David Geffen School of Medicine at UCLA, Los Angeles, CA 90095, USA

**HIV-1-infected individuals are treated with lifelong antiretroviral drugs to control the infection. A means to strengthen the antiviral T cell response might allow them to control viral loads without antiretroviral drugs. We report the development of a lentiviral vector-based dendritic cell (DC) vaccine in which HIV-1 antigen is co-expressed with CD40 ligand (CD40L) and a soluble, high-affinity programmed cell death 1 (PD-1) dimer. CD40L activates the DCs, whereas PD-1 binds programmed death ligand 1 (PD-L1) to prevent checkpoint activation and strengthen the cytotoxic T lymphocyte (CTL) response. The injection of humanized mice with DCs transduced with vector expressing CD40L and the HIV-1 SL9 epitope induced antigen-specific T cell proliferation and memory differentiation. Upon HIV-1 challenge of vaccinated mice, viral load was suppressed by 2 logs for 6 weeks. Introduction of the soluble PD-1 dimer into a vector that expressed full-length HIV-1 proteins accelerated the antiviral response. The results support development of this approach as a therapeutic vaccine that might allow HIV-1-infected individuals to control virus replication without antiretroviral therapy.**

## INTRODUCTION

Combination antiretroviral therapy (cART) lowers HIV-1 loads in patients to undetectable levels but does not cure the infection. Upon cessation of treatment, rare, long-lived, latently infected T cells reseed the infection, leading to virus rebound.[1–5] Escape variants dominate the latent reservoir, and the immune system fails to suppress virus replication.[6] A rare class of elite controllers mount strong antiviral T cell responses and maintain undetectable viral loads without antiretroviral therapy, demonstrating the ability of the immune system to control viral replication.[7–9] Thus, a means to enhance the antiviral immune response during cART might allow patients to discontinue treatment while maintaining suppression of virus replication.

HIV infection induces immune dysfunction in lymphoid and non-lymphoid lineages, impairing cellular and humoral responses. Chronic antigen stimulation leads to the exhaustion of HIV-specific T cells, resulting in the loss of effector function and an inability to produce effector cytokines.[10,11] Immune checkpoint receptors, such as programmed cell death 1 (PD-1) and lymphocyte-activation gene 3, are expressed at increased levels on T cells in chronic HIV-1 infection, which upon engagement further impair T cell cytolytic and proliferative potential. Increased PD-1 expression on HIV-specific T cells correlates with advanced cellular dysfunction and disease progression,[12–15] suggesting that checkpoint engagement is an important regulator of immune exhaustion in HIV-infection. In the treatment of cancer, the use of checkpoint inhibitors such as anti-PD-1 and anti-programmed death ligand 1 (anti-PD-L1) antibodies has resulted in remissions in melanoma, non-small cell lung cancer, renal cell carcinoma, and other solid tumors.[16–22] A soluble PD-1 "microbody" in which a high-affinity PD-1 extracellular domain is fused to an immunoglobulin CH3 domain was shown to bind PD-L1 on effector T cells, preventing PD-1 signaling.[23] In a mouse colon cancer model, the microbody reversed T cell exhaustion and suppressed tumor growth.[23] In HIV-infected patients, anti-PD-L1 antibody was found to enhance HIV-1-specific immunity.[24]

Dendritic cell (DC) vaccines that exploit the ability of the cells to initiate T cell responses have been explored as a means to enhance T cell responses to cancer and other chronic diseases, including HIV-1.[25–28] In DC vaccine strategies, patient monocytes are isolated from peripheral blood mononuclear cells (PBMCs) and differentiated in culture to monocyte-derived DCs (MDDCs) and then pulsed with synthetic peptide epitopes, tumor whole-cell extract, or viral lysate, or alternatively, electroporated with antigen-encoding synthetic mRNA. The treated cells are activated with a cocktail of cytokines and then re-infused. In the patient, DCs presenting antigen on major histocompatibility complex class I (MHC class I) activate antigen-specific cytotoxic T lymphocytes (CTLs). A meta-analysis of 12 clinical trials in which DC-based vaccine strategies were tested for their ability to

Received 12 December 2018; accepted 1 March 2019;
https://doi.org/10.1016/j.ymthe.2019.03.008.

[4]These authors contributed equally to this work.

**Correspondence:** Nathaniel R. Landau, PhD, Department of Microbiology, NYU Langone Medical Center, 430 East 29th Street, Alexandria West Building, Room 509, New York, NY 10016, USA.
**E-mail:** nathaniel.landau@med.nyu.edu
**Correspondence:** Scott Kitchen, PhD, Department of Medicine, Division of Hematology and Oncology, The David Geffen School of Medicine at UCLA, 615 Charles E. Young Drive South, 173 BSRB, Los Angeles, CA 90095, USA.
**E-mail:** skitchen@ucla.edu

 © 2019 The American Society of Gene and Cell Therapy.

boost anti-HIV-1 immune responses showed that the vaccines induced measurable T cell responses and caused the transient suppression of peripheral viral loads.[25]

A limitation in these approaches is that of short-term antigen presentation provided by peptide pulsing or exogenous antigen-loading strategies. To improve the DC vaccine approach, we developed a lentiviral vector-based DC vaccine strategy.[29] In this strategy, the DCs are transduced with a lentiviral vector that encodes the antigen. This strategy provides long-term, endogenous antigen expression, efficient MHC class I antigen presentation, and allows for the co-expression of immunostimulatory cytokines or immune receptors. To achieve high-efficiency DC transduction, we developed a method to generate lentiviral vector stocks that package the simian immunodeficiency virus (SIV) accessory protein Vpx.[30] Upon virus entry, the packaged Vpx induces the proteasomal degradation of the myeloid host restriction factor SAMHD1,[31–34] providing a nearly 2-log increase in DC transduction efficiency.[35] The vectors were produced using the Gag/Pol packaging plasmid pMDL-X in which the Vpx-packaging motif was introduced into the P6 region of Gag. Lentiviral vector stocks were produced by cotransfection of 293T cells with pMDL-X, a codon-optimized Vpx expression vector and the transfer vector.

We previously reported on lentiviral vectors that expressed the immunodominant human leukocyte antigen (HLA)-A*0201-restricted epitope derived from the HIV-1 matrix protein SL9.[29] The vectors co-expressed CD40 ligand (CD40L), a protein of activated T cells that binds to CD40 on DCs to induce their maturation and activate antigen presentation pathways.[36] Transduction of DCs with the vector induced expression of costimulatory proteins CD83 and CD86, and the secretion of high levels of the Th1 cytokine interleukin (IL)-12p70 and the proinflammatory cytokines tumor necrosis factor alpha (TNF-α) and IL-6 without inducing the inhibitory cytokine IL-10. The transduced DCs presented SL9 to an HLA-A*0201-restricted SL9-specific CTL clone and stimulated the expansion of antigen-specific primary CD8 T cells. Coculture of the transduced DCs with HIV-1 latently infected ACH-2 and J-Lat cells induced the expression of the latent provirus, an activity attributed to TNF-α produced by the transduced DCs. The ability of the transduced DCs to activate latent provirus expression is analogous to that of the latency reversing agents currently under development in virus eradication strategies.[37,38]

In this report, we tested the DC vaccine strategy in the humanized bone marrow-liver-thymus (BLT) mouse model for the ability of transduced DCs to elicit a T cell response that suppresses HIV-1 replication. The injection of DCs transduced with vector that expressed CD40L and SL9 induced a strong SL9-specific T cell response and T cell memory. Upon infection of the vaccinated mice with HIV-1, virus load was suppressed 100-fold for up to 6 weeks. A vector expressing full-length HIV-1 proteins and the PD-1 microbody induced an accelerated protective immune response and increased the functionality of the responding CTLs. The results support the development of this approach for therapeutic vaccination of HIV-infected patients.

## RESULTS

To test the ability of transduced DCs to induce an anti-HIV-1 T cell response and to suppress HIV-1 replication *in vivo*, we used the humanized BLT mouse model in which non-obese diabetic-severe combined immunodeficiency (NOD-SCID)-common γ-chain knockout mice are transplanted with human fetal liver, thymus, and bone marrow tissue to reconstitute a functional human immune system.[39,40] The mice support HIV replication and mount CD4 and CD8 T cell responses. Upon infection, plasma virus loads rapidly rise to a set point after which the peripheral blood and lymphoid organ CD4 T cells are gradually depleted.[41] The response of HLA class I-restricted CD8 T cells resembles that in humans in which immunodominant T cell hierarchies are formed.[42,43] For the analysis of the response to the HLA-A*0201-restricted immunodominant HIV-1 Gag epitope SL9, mice were generated with fetal HLA-A*0201$^+$ donor tissue. To provide a source of naive MHC class I-restricted anti-SL9 CD8 T cells, a fraction of the CD34$^+$ hematopoietic stem cells (HSCs) used in the reconstitution was transduced with a vector encoding an SL9-specific human T cell receptor (TCR).[44–46] Analysis of the PBMCs by flow cytometry showed that >60% of the lymphocytes in the BLT mice were of human origin (Figure S1).

### Vector-Encoded CD40L Induces HSC-DC Maturation and Activation

As vaccine vectors that would induce a CD8 T cell response to HIV-1, we constructed the lentiviral vector CD40L-SL9, which encodes SL9 and CD40L, a T cell-expressed protein that engages CD40 on DCs to induce their maturation and activation. As controls, we constructed variants encoding a nonfunctional T147N CD40L (mutant CD40L [mtCD40L])[47] and the lentiviral vector CD40L-M1, which expresses the influenza virus HLA-A*0201-restricted M1 epitope (Figure 1A).[48] SL9 and M1 epitopes in the vectors are expressed as fusions to the C terminus of CD40L with an intervening P2A self-cleaving motif,[49] a configuration that takes advantage of the type II transmembrane topology of CD40L. Upon biosynthesis, the nascent peptide epitope is released into the endoplasmic reticulum lumen for assembly with MHC class I protein and efficient antigen presentation. To increase their titer on DCs, viral vector stocks containing the SIV Vpx accessory protein were produced using the pMDL-X Gag/Pol packaging vector and the Vpx expression vector, and pseudotyped with VSV-G.

As a source of autologous human DCs for use in the humanized mouse model, we sorted CD34$^+$ cells from fetal liver and differentiated the cells in medium containing granulocyte-macrophage colony-stimulating factor (GM-CSF) and stem cell factor (SCF) to CD11c$^+$ HSC-DCs.[50] HSC-DCs could be expanded 100-fold over 2–3 weeks in culture (Figure S2A), providing a large number of DCs for *ex vivo* transduction. The transduction frequency of HSC-DCs with Vpx-containing vectors was 43.7%–68% as determined by the percentage of CD40L$^+$ HSC-DCs (Figure 1B), a range similar to

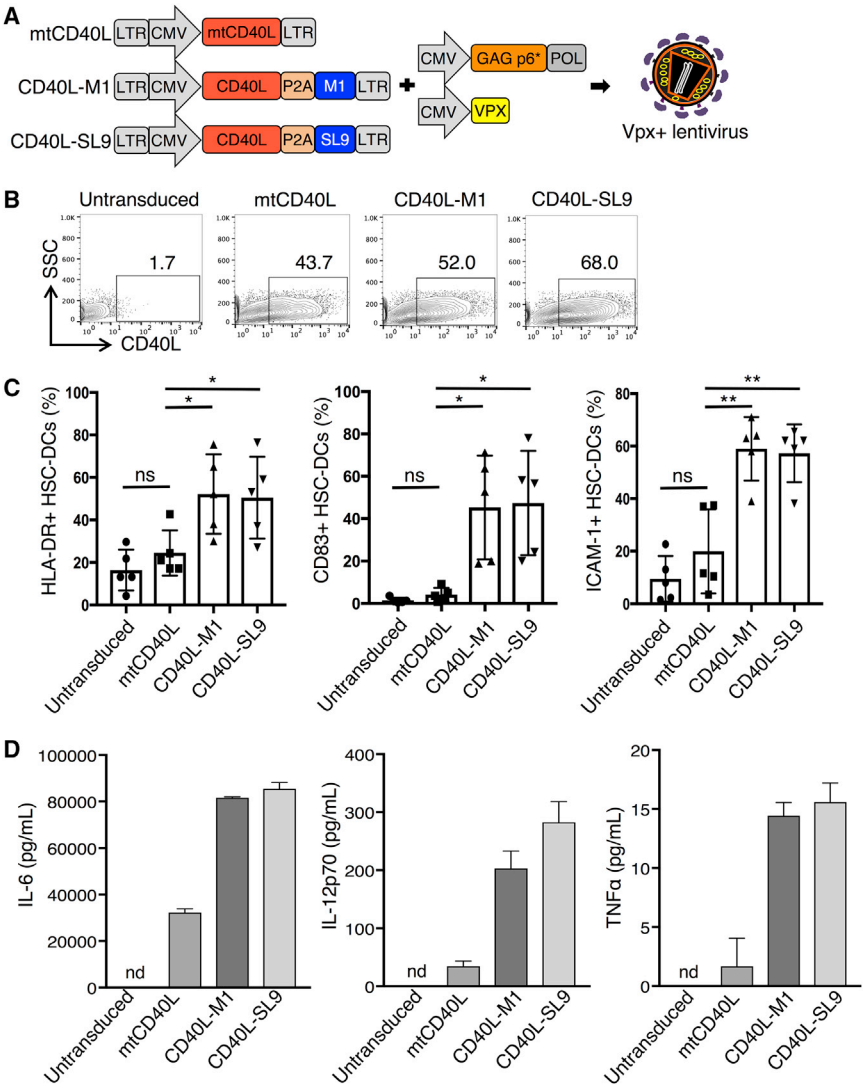


**Figure 1. Vpx-Containing Lentiviral Vectors Expressing CD40L Efficiently Transduce and Activate HSC-DCs**

(A) Diagrams of the ~5.2-kb lentiviral vectors expressing mutant CD40L (mtCD40L), CD40L-M1, or CD40L-SL9 and the Vpx motif chimeric Gag/Pol and SIVmac Vpx expression vectors used to produce Vpx-containing virions are shown. 293T cells cotransfected with the vectors and expression vectors for VSV-G and HIV-1 Rev (not shown) yield Vpx-containing lentiviral vector stocks. (B) HSC-DCs were transduced with the Vpx-containing lentiviral vectors and after 72 h stained with anti-CD40L-PE and analyzed by flow cytometry to determine the percentage of CD40L$^+$ cells. The results shown are representative of three different donor HSC-DCs. (C) The expression of HLA-DR, CD83, and ICAM-1 on the transduced HSC-DCs was quantified by flow cytometry. Pooled results from five donors are shown. Data represent mean ± SD. *$p < 0.05$, **$p < 0.01$ by unpaired two-tailed t test with Welch's correction. (D) IL-6, IL-12p70, and TNF-α in the transduced HSC-DC supernatant were quantified by cytokine bead array. Data represent triplicate samples from one donor with mean ± SD. nd, not detected. Additional donors are shown in Figure S2C.

that achieved in the transduction of human MDDCs.[29] CD40L induced the HSC-DCs to express HLA-DR, CD83, and ICAM-1 (Figures 1C and S2B) and secrete high levels of IL-6, IL-12p70, and TNF-α (Figures 1D and S2C). Vectors expressing mtCD40L with or without the SL9 epitope had no effect. The findings demonstrate the ability of CD40L-expressing vectors to cause HSC-DCs to mature and become activated.

### CD40L-SL9-Transduced HSC-DCs Elicit SL9-Specific T Cell Responses in Humanized Mice

To test the ability of lentiviral vector-transduced HSC-DCs to induce an immune response to HIV, SL9 TCR BLT mice were injected intravenously (i.v.) with $1 \times 10^6$ autologous CD40L-SL9-transduced HSC-DCs (Figure 2A) and then bled weekly to quantify the SL9 TCR$^+$ CD8 T cells. The results showed that 1 week post-injection, the frequency of SL9 TCR$^+$ CD8 T cells increased from 1.4% to 13.7% (Figure 2B). In an experiment using n = 5, the frequency of SL9 TCR$^+$ CD8 T cells increased by 0.5–2 logs (Figure 2C). The frequency did not increase in mice injected with control untransduced HSC-DCs, demonstrating the SL9 antigen specificity of the response. To determine the phenotype of the responding T cells, we analyzed the CD8 T cells of the vaccinated mice for CD45RA, CD62L, and SL9 TCR to define SL9 TCR$^+$ and SL9 TCR$^-$ CD8 T cell subsets as naive (CD45RA$^+$/CD62L$^+$), effector memory (EM; CD45RA$^-$/CD62L$^-$), and central memory (CM; CD45RA$^-$/CD62L$^+$). Results showed that SL9 TCR$^-$ CD8 T cells were 61% naive (CD45RA$^+$) and 39% memory (CD45RA$^-$) with 9% EM and 30% CM (Figure 2D). The SL9 TCR$^+$ CD8 T cells consisted of fewer naive cells (26%) and a larger proportion of memory cells (26% EM and 49% CM). A pooled analysis showed that in the vaccinated mice, 80% of the SL9 TCR$^+$ T cells became memory cells, whereas in control mice, the proportion of SL9 TCR$^-$ and SL9 TCR$^+$ memory CD8 T cell populations was unchanged (Figure 2E). Analysis of the activation state of the responding T cells by CD69 expression showed that at 1 week post-CD40L-SL9 vaccination, SL9 TCR$^+$ CD8 T cells became activated, whereas SL9 TCR$^-$ CD8 T cells did not, the latter serving as an internal control for the antigen specificity of activation (Figure 2F). Moreover, CD69 was not induced in the SL9 TCR$^+$ CD8 T cells of control mice (Figure 2G). Taken together, the findings suggest that the injection of CD40L-SL9-transduced HSC-DCs induced antigen-specific CD8 T cell proliferation and established effector and CM CD8 T cells that were dependent upon expression of both CD40L and SL9, consistent with our prior *in vitro* studies using MDDCs.[29]

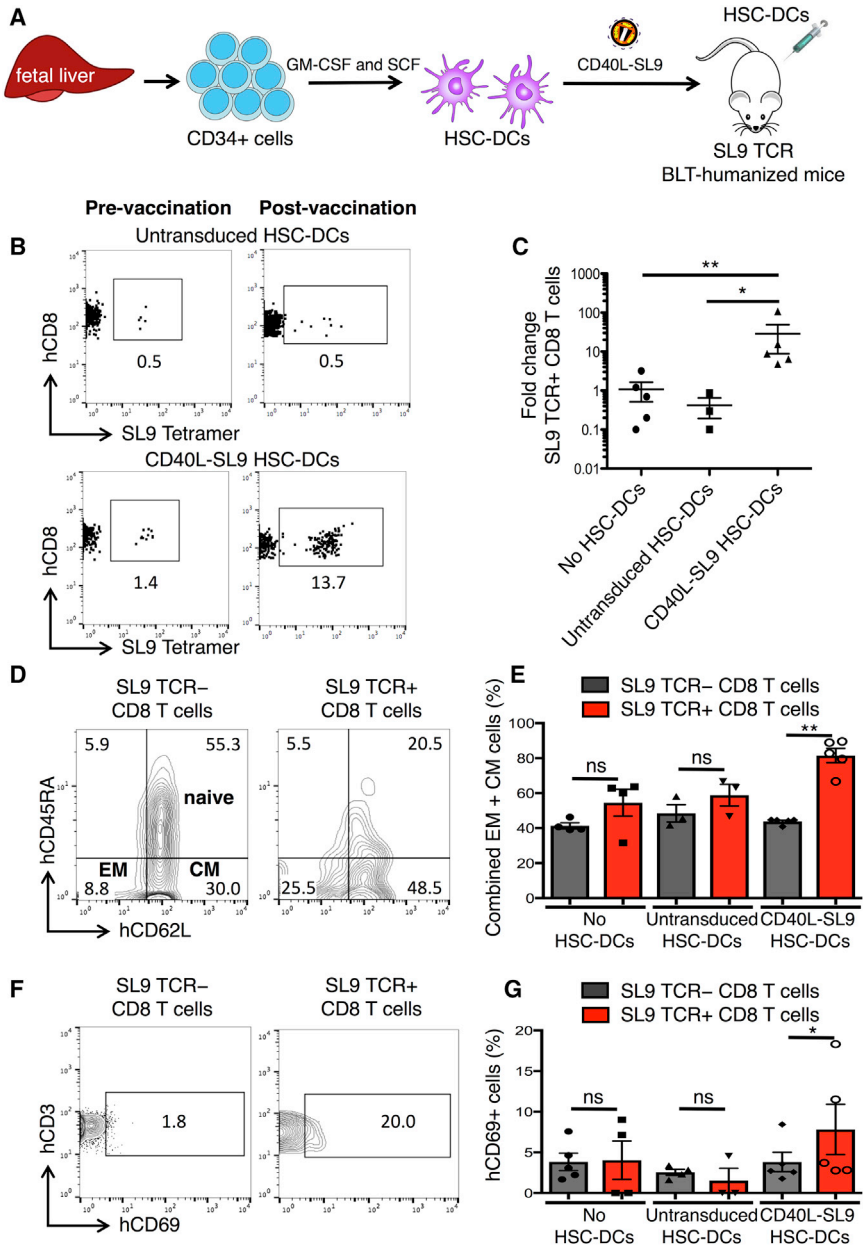


**Figure 2. Vector-Transduced HSC-DCs Induce Expansion and Differentiation of SL9 TCR$^+$ CD8 Cells in Humanized Mice**

(A) SL9 TCR humanized BLT mice were generated by implanting fetal liver, thymus, and SL9 TCR-transduced HSCs in matrigel under the renal capsule while in parallel injecting SL9 TCR-transduced HSCs retro-orbitally. Eight weeks after engraftment, autologous CD34$^+$ fetal liver stem cells were differentiated and expanded in culture to HSC-DCs that were then transduced with CD40L-SL9 and injected into the SL9 TCR-BLT mice (n = 5). Unvaccinated mice and those injected with untransduced HSC-DCs served as controls. (B) One week post-vaccination, the percentage of human CD45$^+$, CD3$^+$, CD8$^+$ SL9 TCR$^+$ cells was determined by flow cytometry. Representative plots pre- and post-vaccination with untransduced or CD40L-SL9-transduced HSC-DCs are shown. (C) The ratio of SL9 TCR$^+$ CD8 T cells post-vaccination:pre-vaccination is shown for each group. Data represent mean ± SEM. *p < 0.05, **p < 0.01 by Mann-Whitney U tests. (D) One week post-vaccination, the percentages of naive (CD45RA$^+$/CD62L$^+$), effector memory (EM; CD45RA$^-$/CD62L$^-$), and central memory (CM; CD45RA$^-$/CD62L$^+$) SL9 TCR$^-$ and SL9 TCR$^+$ CD8 T cell subsets were determined by flow cytometry. Representative plots from a CD40L-SL9-vaccinated mouse are shown. (E) Pooled analysis of the SL9 TCR$^-$ (gray) and SL9 TCR$^+$ (red) EM and CM CD8 T cells is shown. Data represent mean ± SD. *p < 0.05, **p < 0.01 by Wilcoxon matched-pairs signed rank tests. (F) SL9$^+$ TCR$^-$ and SL9$^+$ TCR$^+$ subsets were analyzed for human CD3 and CD69 by flow cytometry. Representative plots from a CD40L-SL9-vaccinated mouse are shown. (G) Pooled analysis of the percentage of CD69$^+$ SL9 TCR$^-$ (gray) and SL9 TCR$^+$ (red) CD8 T cells is shown. Data represent mean ± SD. *p < 0.05, **p < 0.01 by Wilcoxon matched-pairs signed rank tests.

### CD40L-SL9 Vector-Transduced HSC-DCs Suppress HIV-1 Replication *In Vivo*

To determine the ability of the vaccine to suppress HIV-1 replication *in vivo*, HLA-A*0201 SL9-TCR BLT humanized mice were injected with CD40L-SL9-transduced HSC-DCs and 3 weeks later, they were challenged with an infectious HIV-1 that expresses the SL9 epitope. Analysis of the CD8 T cells post-vaccination, but prior to HIV-1 challenge, showed that vaccination caused a transient increase in the fraction of SL9 TCR$^+$ CD8 T cells that returned to baseline after 3 weeks (Figure 3A). Upon HIV-1 challenge, in unvaccinated control mice, the percentage of SL9 TCR$^+$ CD8 T cells increased in only one of the five mice. The results were similar in mice vaccinated with control HSC-DCs. In contrast, in CD40L-SL9-vaccinated mice, SL9 TCR$^+$ CD8 T cells expanded 10-fold on average, increasing to as much as 30% of the total CD8 T cells in one mouse. Analysis of the viral loads in the mice post-HIV-1 challenge showed high copy numbers of HIV-1 RNA at 2 weeks. At week 4, in unvaccinated and control HSC-DC-vaccinated mice, viral loads were unchanged, whereas in mice injected with CD40L-SL9-transduced HSC-DCs, viral loads decreased 4-fold. By week 6, in unvaccinated and control HSC-DC-vaccinated mice, viral loads increased 10-fold. In contrast, in mice injected with CD40L-SL9-transduced HSC-DCs, viral loads decreased 10-fold, resulting in more than a 2-log difference in viral load on average between vaccinated and control mice at 6 weeks post-infection (Figure 3B). The suppression was transient, returning to close to the set point at 8 weeks.

A potential explanation for rebound of the viral load was the emergence of viral escape mutants; however, nucleotide sequence

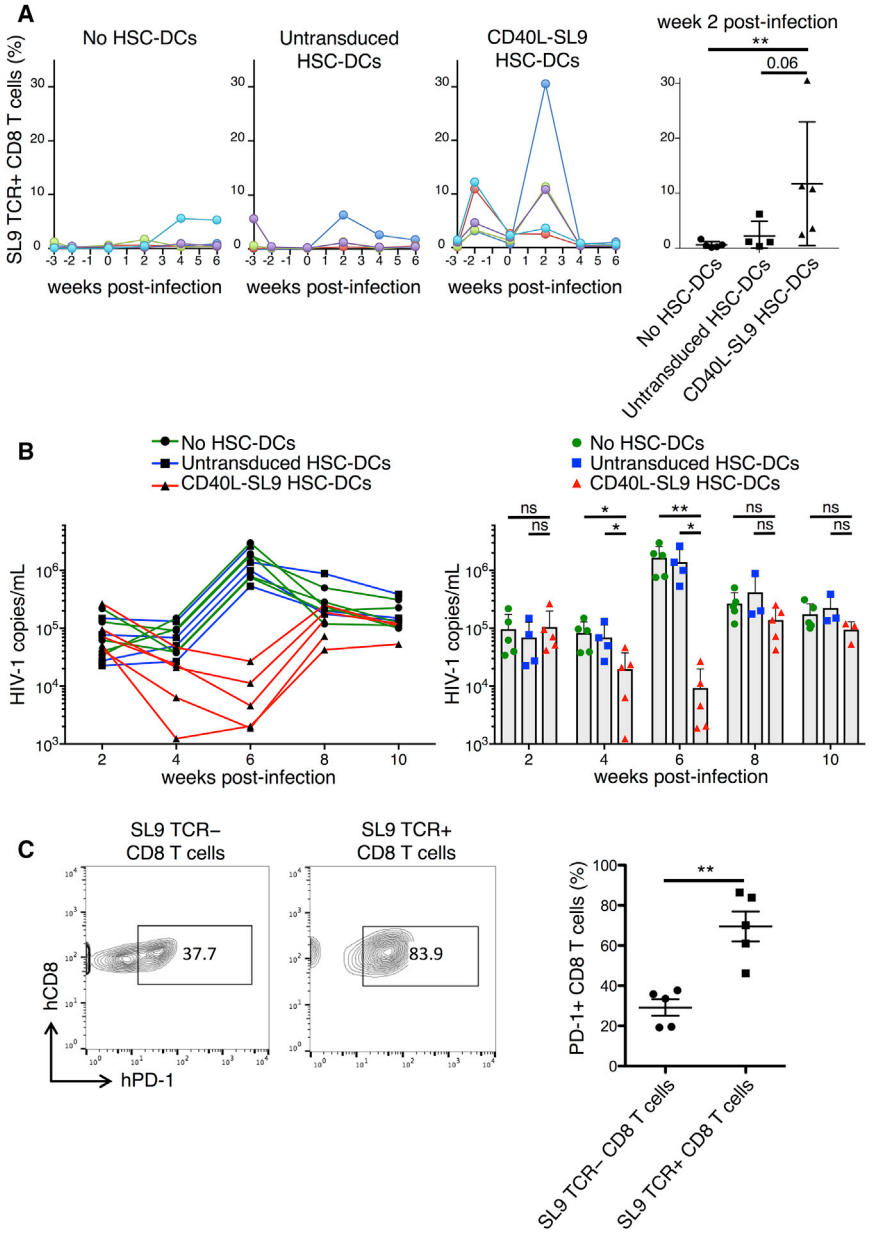


**Figure 3. Suppression of HIV-1 Replication in Vaccinated BLT Mice**

BLT mice were unvaccinated (no HSC-DCs) or injected with untransduced or CD40L-SL9-transduced HSC-DCs and 3 weeks later challenged with HIV-1. (A) The frequency of SL9 TCR$^+$ CD8 T cells was determined pre- and post-vaccination over 10 weeks. Each line represents an individual mouse, n = 4–5 per group. Pooled analysis at 2 weeks post-HIV-1 infection is shown on the right. Data represent mean ± SD. **p < 0.01 by Mann-Whitney U tests. (B) Individual viral loads in the peripheral blood of the unvaccinated and vaccinated mice are shown. Pooled analysis is shown on the right. Data represent mean ± SD. *p < 0.05, **p < 0.01 by Mann-Whitney U tests. (C) After 10 weeks, the relative amount of PD-1 on SL9 TCR- and SL9 TCR$^+$ CD8 T cell subsets in CD40L-SL9 vaccinated mice was measured by staining for human CD45, CD3, CD8, PD-1, and SL9 tetramer. Representative plots from one mouse (left) and pooled analysis from five mice (right) are shown. Data represent mean ± SEM. **p < 0.01 by Wilcoxon matched-pairs signed rank tests.

analysis of virion and cell-associated RNA in the region of the viral genome containing the SL9 coding sequence 12 weeks post-HIV-1 challenge showed no increase in the frequency of mutations (Figure S3). Another possibility was that the rebound was caused by CTL exhaustion, a phenomenon that occurs in chronic viral infections, including HIV-1, which is mediated by signaling through PD-1/PD-L1 and other checkpoint receptors.[10,11,13,51] Analysis 10 weeks post-infection of the vaccinated mice showed that the fraction of PD-1$^+$ SL9 TCR$^+$ CD8 T cells increased compared with the fraction of PD-1$^+$ SL9 TCR$^-$ CD8 T cells (Figure 3C), rendering them susceptible to checkpoint activation by PD-L1.

### PD-1 Microbody-Expressing HIV-Based Vector Accelerates the Antiviral Response

To generate a lentiviral vector that would increase the number of responding T cells and prevent checkpoint activation, we constructed pHIV.PD1-CD40L, a vector that expresses full-length *gag*, *pol*, *vif*, *rev*, and *tat*, but is deleted for *vpu* and most of *env*, and has a Vpx packaging motif sequence in Gag P6. In place of *nef*, the vector has a cytomegalovirus (CMV) promotor-driven cassette that encodes CD40L and a PD-1 "microbody" (Figure 4A) in which the extracellular domain of PD-1 is fused to an immunoglobulin heavy-chain constant region and has an amino-terminal his-tag.[23] The protein binds to PD-L1 with high affinity, blocking the interaction with T cell PD-1 to prevent T cell checkpoint activation.[23]

To test for production of the microbody by the vector, 293T cells were transduced with HIV.PD1-CD40L, and the protein was pulled down from the supernatant by immobilized metal affinity chromatography. Controls included lentiviral vectors encoding GFP (control LV), the PD-1 microbody fused to mtCD40L or CD40L (PD1-mtCD40L and PD1-CD40L), or a poly-HIV-1 antigen vector expressing GFP (HIV.GFP). Immunoblot analysis showed that cells transduced with HIV.PD1-CD40L, PD1-CD40L, or PD1-mtCD40L produced the microbody (Figure 4B). The HIV.PD1-CD40L vector produced less PD-1 microbody than the lentiviral vectors despite being added at the same MOI and driven by the same CMV promoter. A possible explanation for this is that in the lentiviral vectors, the LTR and CMV promoters are

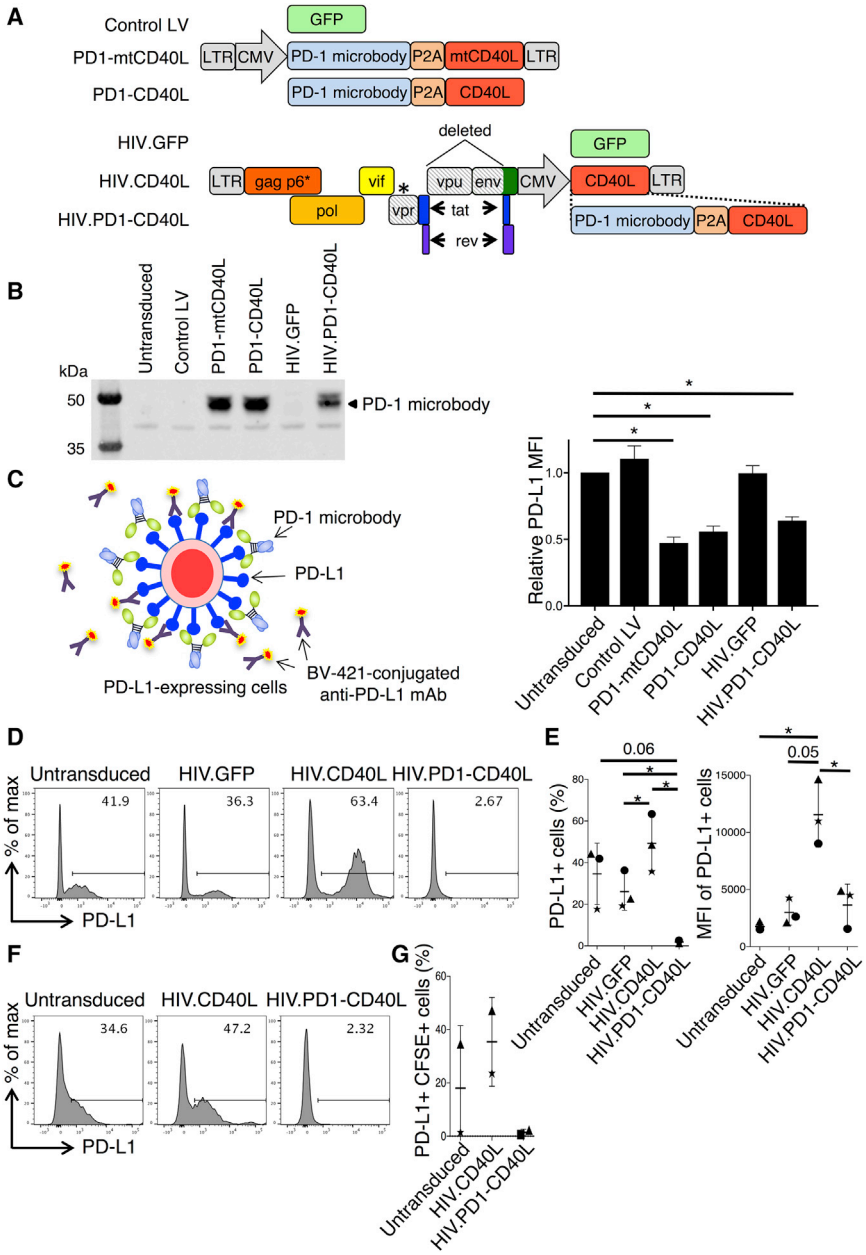


**Figure 4. Lentiviral Vector-Encoded PD-1 Microbody Binds with High Affinity to PD-L1**

(A) Lentiviral vectors expressing GFP (control LV) or PD-1 microbody fused to mutated or wild-type CD40L (PD1-mtCD40L or PD1-CD40L) via a P2A sequence are diagrammed (top). NL4-3-based vectors containing the SIV Vpx-packaging motif in p6, a stop codon in *vpr* (*), and deletions in *vpu* and *env* (diagonal shading) are shown (bottom). A cassette expressing CMV-driven GFP (HIV.GFP), CD40L (HIV.CD40L), or PD1-CD40L (HIV.PD1-CD40L) replaces *nef*. Lentiviral vector constructs are 5.1–6.1 kb. HIV vector constructs are 9.7–10.8 kb. (B) 293T cells were transduced with the vectors, and after 72 h supernatant PD-1 microbody was quantified by immunoblot. (C) Diagram of competitive binding assay in which PD-1 microbody binds PD-L1 on 293T.PDL1 cells, preventing the binding of anti-PD-L1 antibody (left). 293T.PDL1 cells were cultured with supernatant from vector-transduced 293T cells, and PD-L1 expression was measured by flow cytometry (right). Data pooled from two separate experiments normalized to PD-L1 MFI of 293T.PDL1 cells cultured with untransduced 293T cell supernatant are shown. Data represent mean ± SD. *$p < 0.05$ by paired t tests. (D) MDDCs were untransduced or transduced with HIV.GFP, HIV.CD40L, and HIV.PD1-CD40L vectors, and after 72 h the percentage of PD-L1$^+$ cells was determined by flow cytometry. Representative plots are shown. (E) The percentage of PD-L1$^+$ cells (left) and their corresponding MFI (right) from three donors are shown. Data represent mean ± SD. *$p < 0.05$ by paired t test. (F) CFSE-labeled MDDCs were cultured with autologous untransduced or HIV.CD40L or HIV.PD1-CD40L-transduced MDDCs, and the percentage of CFSE$^+$ PD-L1$^+$ cells was determined by flow cytometry. Representative plots are shown. (G) Pooled data from two donors are shown. Data represent mean ± SD.

adjacent and this dual-promoter-enhancer drives higher expression than the HIV.PD1-CD40L vector, where expression is driven by the CMV promoter alone. To test the ability of the microbody to block cell surface PD-L1, the supernatants were incubated with 293T.PDL1 cells that stably express PD-L1, and the cells were then stained with fluorescent anti-PD-L1 antibody and analyzed by flow cytometry. Microbody binding to PD-L1 blocks access to the anti-PD-L1 antibody, resulting in a negative correlation with fluorescence intensity. The results confirmed that the vector-produced PD-1 microbody binds with high affinity to PD-L1 (Figure 4C).

To test the ability of the vector to block PD-L1 on DCs that would be used in clinical application of the vaccine approach, donor MDDCs were transduced with HIV.PD1-CD40L and control HIV.GFP or HIV.CD40L vectors and after 3 days, they were analyzed for PD-L1 expression. Of the untransduced DCs, 41.9% were PD-L1$^+$, and the expression was unaffected by transduction with control HIV.GFP. Transduction with HIV.CD40L caused an increase to 63% PD-L1$^+$ DCs that was accompanied by a 5-fold increase in mean fluoresence intensity (MFI), suggesting that CD40L strongly induced PD-L1 expression in the DCs. Interestingly, transduction with HIV.PD1-CD40L completely prevented staining with the anti-PD-L1 antibody, suggesting that the microbody efficiently blocked access of the antibody to PD-L1 (Figure 4D). Results from the analysis of three donor DC preparations are shown (Figure 4E), and similar results were obtained with HSC-DCs (Figure S4). To test whether the PD-1 microbody could act at a distance on bystander DCs, we

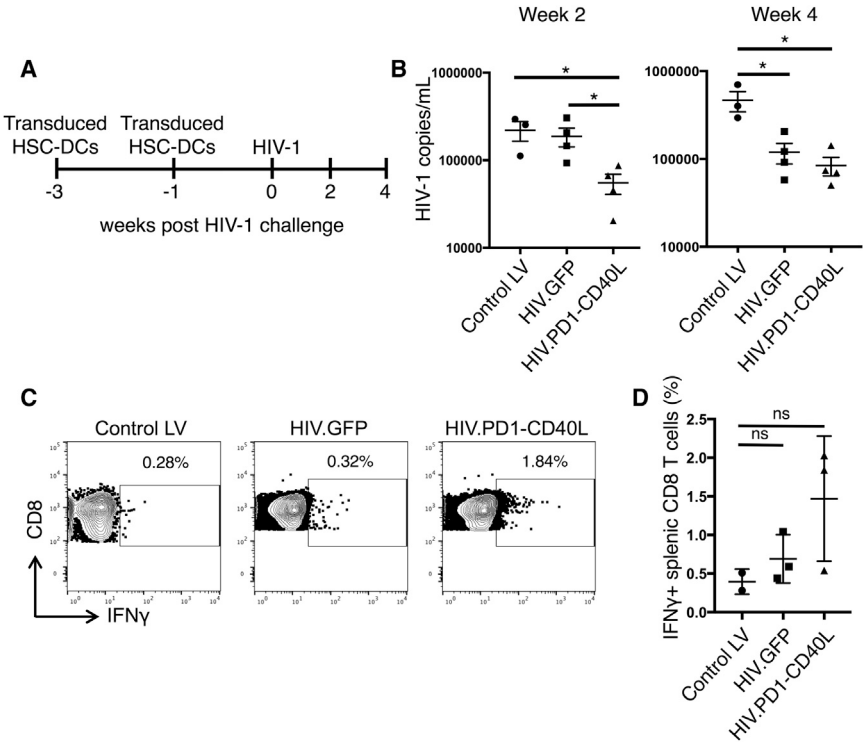


**Figure 5. HIV.PD1-CD40L Vector Expressing PD-1 Microbody and CD40L Strengthens the Antiviral Response**

(A) BLT humanized mice were injected with empty vector (control LV), HIV.GFP, or HIV.PD1-CD40L-transduced HSC-DCs twice over a 2-week period and 1 week later challenged with HIV-1 (n = 3–4). A timeline is shown. (B) At week 2 (left) and week 4 (right) post-HIV-1 challenge, peripheral HIV-1 loads were determined by qRT-PCR. Pooled data are shown. Data represent mean ± SEM. *$p < 0.05$ by Mann-Whitney U tests. (C) At week 4 post-HIV-1 challenge, mouse splenocytes were pulsed with a pool of clade B HIV-1 peptides, and the percentage of IFN$\gamma^+$ T cells was determined by intracellular staining and flow cytometry. Representative plots from one mouse per group are shown. (D) Pooled analysis of the mice is shown (n = 2 for control LV, n = 3 for HIV.GFP and HIV.PD1-CD40L). Data represent mean ± SD. Significance was determined by Mann-Whitney U tests.

labeled MDDCs with carboxyfluorescein succinimidyl ester (CFSE) and co-cultured them with unlabeled control or HIV.CD40L- or HIV.PD1-CD40L-transduced MDDCs and then analyzed PD-L1 on the CSFE-labeled MDDCs. Coculture with CD40L-expressing MDDCs caused the bystander CSFE-stained MDDCs to induce PD-L1, whereas coculture with MDDCs expressing CD40L and the PD-1 microbody completely blocked access of the anti-PD-L1 antibody to PD-L1 (Figures 4F and 4G). The results demonstrated that the PD-1 microbody expressed by HIV.PD1-CD40L-transduced DCs acts both in *cis* and *trans* to block access to PD-L1. Immunoblot analysis of HIV.PD1-CD40L vector-transduced MDDCs showed that they synthesized HIV-1 Gag (Figure S5A). Moreover, the MDDCs secreted high levels of TNF-$\alpha$ (Figure S5B) and increased their cell surface CD83 (Figure S5C). These findings suggest that HIV.PD1-CD40L-transduced MDDCs could present antigen to anti-HIV T cells and prime an immune response in the absence of PD-L1-mediated checkpoint activation.

To evaluate the ability of HIV.PD1-CD40L-transduced DCs to induce a protective immune response, we vaccinated BLT humanized mice. Because the vector encodes many T cell epitopes, there was no need to use mice reconstituted with HLA-A*0201 human tissue or to supplement with SL9 TCR-transduced stem cells. To vaccinate the BLT mice, HSC-DCs were transduced with HIV.PD1-CD40L, HIV.GFP, or empty vector control (control LV) and injected twice over a 2-week period. One week later, the mice were challenged with HIV-1 (Figure 5A). HIV.PD1-CD40L-transduced HSC-DCs caused a 5-fold reduction in viral load 2 weeks post-challenge and a 10-fold reduction 4 weeks post-challenge (Figure 5B). HSC-DCs transduced with HIV.GFP, which encodes HIV-1 antigens but lacks PD-1 and CD40L, also caused a reduction in viral load, but this was not as rapid. To determine the number of responding T cells, an *in vitro* T cell activation assay was used in which splenocytes from the vaccinated mice were pulsed with a pool of clade B peptides spanning the viral protein coding sequence, and the responding interferon $\gamma^+$ (IFN$\gamma^+$) CD8 T cells were quantified by flow cytometry. Vaccination with HIV.PD1-CD40L induced a 4-fold increase in responding T cells, whereas HIV.GFP had only a nominal effect (Figure 5C and pooled analysis in Figure 5D). The results suggest that the vaccination induced a suppressive immune response that was enhanced by the combination of PD-1 microbody and CD40L.

To determine the relative contribution of CD40L and the PD-1 microbody to virus load suppression, we compared the ability of vectors expressing CD40L (HIV.CD40L) or the PD-1 microbody and mtCD40L (HIV.PD1-mtCD40L) to suppress virus loads in BLT humanized mice. HSC-DCs were transduced, injected into the mice, and 1–2 weeks later, the mice were infected with HIV-1 (Figure 6A). Unlike in Figure 3B, where control mice viral loads peaked at week 4 post-infection, control mice viral loads in this cohort peaked at week 2. The difference in replication kinetics may have been caused by MHC donor haplotype differences in the humanized mice. At 2 weeks post-challenge, vaccination with HIV.CD40L or PD1-mtCD40L caused a 3.5-fold reduction in viral load compared with control, whereas vaccination with HIV.PD1-CD40L induced a 6-fold reduction (Figure 6B). At week 4, HIV.CD40L- and HIV.PD1-CD40L-vaccinated mice further suppressed viral loads as compared with HIV.PD1-mtCD40L-vaccinated mice. Viral loads continued to decline over the next 4 weeks for all of the groups, with the greatest decline in mice vaccinated with HIV.CD40L and

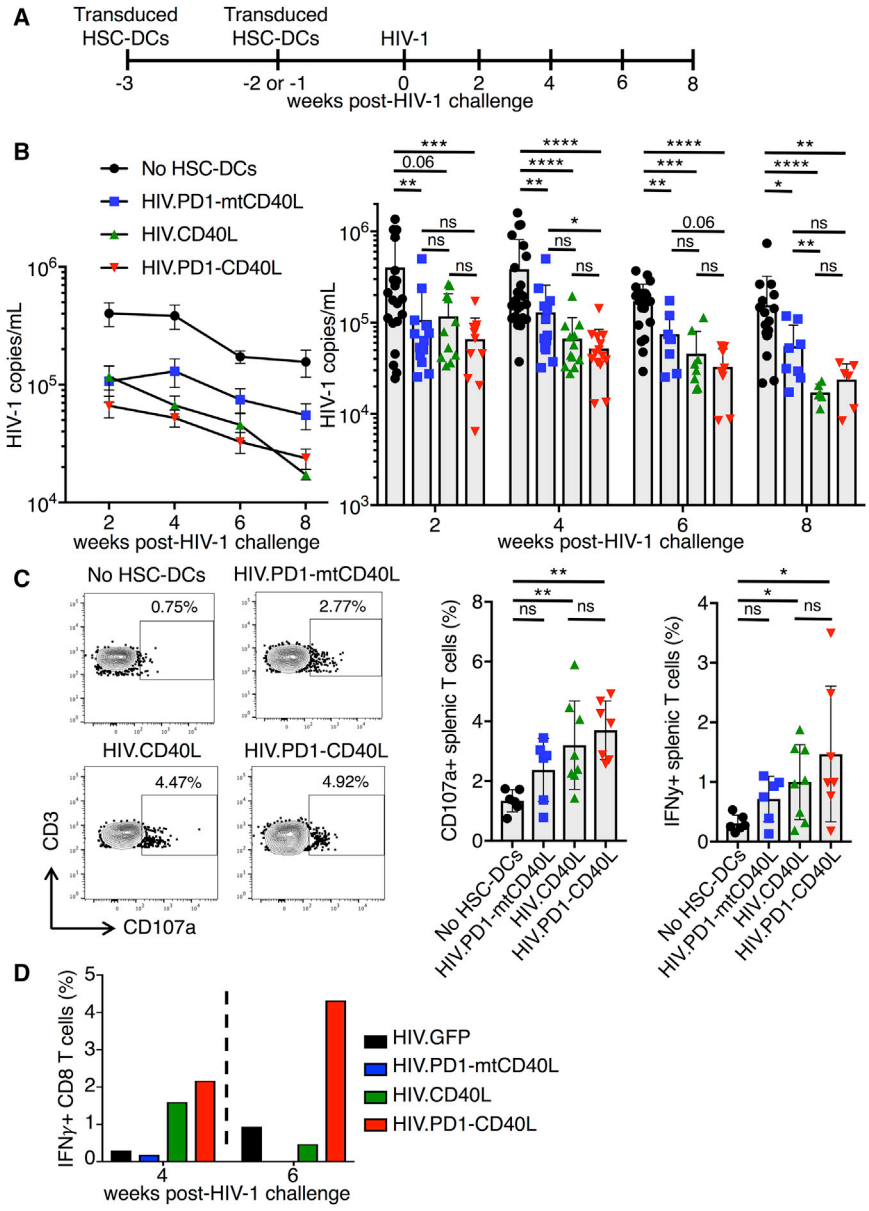


**Figure 6. Vector Expressing CD40L and PD-1 Microbody Provides an Accelerated and More Functional T Response**

(A) BLT mice were injected with empty vector HIV.PD1-mtCD40L, HIV.CD40L, or HIV.PD1-CD40L-transduced HSC-DCs twice over a 2-week period. One week later, the mice were challenged with HIV-1. Results represent aggregate data from three independent experiments in which BLT humanized mice were generated from three different non-HLA-A*0201-restricted donors (n = 6–26/group). (B) Peripheral HIV-1 loads were determined every 2 weeks by qRT-PCR. Pooled data are shown. Line graphs (left) represent mean ± SEM. Bar graphs showing individual mice (right) represent mean ± SD. *$p < 0.05$, **$p < 0.01$ by Mann-Whitney U tests. (C) At week 8 post-HIV-1 challenge, mouse splenocytes were pulsed with a pool of clade B HIV-1 peptides, and the percentage of CD107a$^+$ and IFNγ$^+$ T cells was determined by intracellular staining and flow cytometry. Representative plots from one mouse per group for CD107a expression are shown (left), and pooled analyses of the mice for CD107a and IFNγ expression are shown (right) (n = 5–8/group). Data represent mean ± SD. *$p < 0.05$, **$p < 0.01$ by Mann-Whitney U tests. (D) BLT humanized mice were injected with untransduced HSC-DCs or HIV.GFP, HIV.CD40L, HIV.PD1-mtCD40L, or HIV.PD1-CD40L-transduced HSC-DCs twice over a 2-week period and 1 week later challenged with HIV-1 (n = 4–5/group). At week 4 (left) and week 6 (right) post-HIV-1 challenge, PBMCs from each group were pooled and analyzed as in (C).

HIV.PD1-CD40L, suggesting that CD40L strengthened the immune response.

To measure the effect of the vaccination on T cell function, splenocytes were pulsed with the clade B HIV-1 peptide pool and then stained for IFNγ and CD107a, a marker of CTL activity (Figure 6C). Mice vaccinated with HIV.CD40L and HIV.PD1-CD40L had significant increases in the number of CD107a$^+$ and IFNγ$^+$ T cells compared with controls with no HSC-DCs. The HIV.PD1-CD40L-vaccinated mice appeared to induce a slightly stronger response than HIV.CD40L-vaccinated mice, although the difference was not statistically significant. To test the effect of vaccination on the T cells response at earlier time points, BLT mice were vaccinated and bled 4 and 6 weeks post-HIV challenge. Blood samples were analyzed in pools to provide a sufficient number of cells, and the T cell response to the peptide pool was measured. At week 4 post-HIV-1 challenge, HIV.CD40L and HIV.PD1-CD40L vaccination increased the frequency of IFNγ$^+$ CD8 T cells 5-fold compared with mice immunized with HIV.GFP or HIV.PD1-mtCD40L-transduced HSC-DCs (Figure 6D). At 6 weeks post-HIV-1 challenge, only the HIV.PD1-CD40L-immunized mice maintained a 5-fold increase in the frequency of IFNγ$^+$ CD8 T cells. Taken together, the results show that the combination of PD-1 microbody and CD40L in the antigen-presenting DCs accelerated the T cell response to the HIV antigens and increased the functionality of the responding cells.

## DISCUSSION

We report the development of a therapeutic lentiviral vector-based DC vaccine that generates an antiviral T cell response that suppresses HIV-1 replication in humanized mice. The lentiviral vectors tested encoded HIV-1 antigen and co-expressed CD40L as a means to induce DC maturation and activation, and a PD-1 microbody to prevent checkpoint activation. DCs transduced with a single

epitope-encoding vector induced the activation, proliferation, and differentiation of antigen-specific CD8 T cells. Upon HIV-challenge, virus loads were suppressed by 2 logs for up to 6 weeks post-challenge. A vector that expressed full-length HIV proteins together with CD40L and the PD-1 microbody induced an anti-HIV immune response that suppressed viral loads as early as 2 weeks post-HIV challenge and increased the function of the responding T cells.

The lentiviral vector DC vaccine, by enforcing MHC class I antigen presentation and inducing the activation of DCs, provides a mechanism to counteract the immuno-evasion strategies of HIV-1. HIV-1 infection of unvaccinated BLT mice resulted in only a modest antiviral CD8 T response. Although virus loads climbed to high levels, the frequency of SL9 $TCR^+$ CD8 T cells remained low. The modest response may be because HIV-1, which lacks Vpx, leaves DCs uninfected, dampening the antiviral T cell response,[52–54] and because Nef downregulates MHC class I, minimizing antiviral CTL induction.[55,56] Vaccination of BLT mice with CD40L-SL9 vector-transduced DCs induced antigen-specific CD8 T cells to proliferate and differentiate into EM and CM cells. Activation of the antigen-specific CD8 T cells was driven by DCs that presented antigen on MHC class I and by CD40L that induced their maturation and activation. Vector-expressed CD40L could serve to restore function to DCs, which in chronic infection become dysfunctional as a result of inflammatory factors that induce IL-10 and PD-L1 and the development of immunosuppressive DCs.[40,57]

Viral load suppression induced by vaccination was temporary, with viral loads rebounding by 8 weeks post-challenge. The rebound was not caused by immune escape as shown by the absence of mutations in the rebound virus. A possible explanation is that the transduced DCs have a limited half-life and that once they are gone, the immune response wanes. If this were the case, an additional injection of transduced DCs might prolong the vaccine response. It is also possible that the humanized mouse immune system is not as robust as that in a human. In vaccinated patients, the response may be more durable.

In chronic HIV-1 infection, T cells become exhausted, diminishing the ability of the immune response to suppress virus replication. PD-1 levels in plasma and on HIV-specific T cells are increased, as are PD-L1 levels on monocytes and DCs, both in patients and in infected humanized mice.[15,57,58] Upon initiation of cART, PD-1 levels decrease. In addition, PD-1 levels in elite controllers are lower than those of progressors, findings that suggest that PD-1 levels are maintained by continuous antigen stimulation.[13,59] Checkpoint inhibitors that reverse T cell exhaustion in cancer immunotherapy have been tested in the treatment of HIV and found to partially rescue HIV-1-specific immune responses in patients and overcome T cell exhaustion in HIV-1-infected humanized mice.[24,60,61] An approach that minimizes checkpoint activation on responding T cells would boost the anti-HIV-1 T cell response by allowing unopposed CD28 costimulation of T cells, resulting in more functional effector cells.[62] We found that vectors that expressed the PD-1 microbody accelerated the T cell response and reduced viral loads in humanized mice. Although checkpoint activation is thought of as a late response that induces T cell exhaustion, in the humanized mice, it also acted early post-HIV challenge. It has been shown that PD-1 is induced early in T cell activation, inhibiting the differentiation of effector CD8 T cells.[63] The PD-1 microbody might prevent early induction of PD-1, accounting for the more rapid response in humanized mice. Compared with humanized mice vaccinated with HIV.GFP-transduced DCs that express HIV-1 antigens but lack the PD-1 microbody and CD40L, HIV.PD1-CD40L-transduced DCs accelerated virus suppression and induced more functional HIV-specific T cells, although this was a modest effect. The effect might be greater in chronically infected humanized mice in which HIV-specific CTLs have become exhausted and express high-levels of PD-1. Because the PD-1 microbody is soluble, it could also act on bystander DCs.

"Shock and kill" approaches are being developed to reduce the size of the latent HIV-1 reservoir in infected individuals. In these approaches, patients on cART are treated with a latency reversing agent that activates latent provirus transcription, allowing the cells to be targeted by the adaptive immune system. However, waning of the T cell response during long-term cART renders CTL activity insufficient.[37,64,65] We have shown that vector-transduced DCs themselves can act as a latency reversing agent by secreting high levels of TNF-$\alpha$.[29] By homing to lymphoid areas where latently infected cells reside, transduced DCs could both activate latent provirus transcription and stimulate antiviral CTLs to reduce the latent reservoir.

A concern for this approach is that the transduced DCs could be inflammatory; however, this did not appear to be the case in our experiments. Although the vaccine induced the activation of antigen-specific CD8 T cells, it did not activate antigen-nonspecific SL9 $TCR^-$ CD8 T cells, nor did it increase peripheral levels of TNF-$\alpha$ and IL-6 (data not shown). Moreover, injected DCs have a limited half-life such that potential complications would be temporary.[66]

Incorporation of a checkpoint inhibitor into the vaccine vector provides a means to focus the response on T cells as they interact with antigen-expressing DCs. The approach avoids the autoimmune inflammation that can result from the injection of large doses of monoclonal antibody.[67] Whether the levels of checkpoint inhibitor achieved by transduced DCs are sufficient to have a clinical impact on checkpoint activation remains to be determined. Alternatively, DC vaccination could be coupled with anti-checkpoint therapies, such as anti-PD-1, anti-PD-L1, or anti-CTLA-4 antibody, to induce a systemic checkpoint blockade.

Clinical use of a DC vaccine will require vectors that express more than a single T cell epitope. For this purpose, we tested the HIV.PD1-CD40L vector that expresses full-length HIV proteins. Such a vector broadens the array of responding CTLs and is not restricted to use in HLA-A*0201 haplotype individuals. In clinical use, the effectiveness of the vaccine could be further increased by tailoring the vector to patient-specific viral sequences. Because the vector is based on a deleted HIV-1 provirus, it is not suitable for

use in patients and would require additional attenuating modifications. In this study, we focused on HIV-1; however, the approach is readily adaptable to other purposes, notably cancer immunotherapy, where DC expression of tumor antigens and a checkpoint inhibitor would enhance the anti-tumor T cell response.

## MATERIALS AND METHODS

### Plasmids

To construct pLenti.CD40L, CD40L cDNA was generated from human lymphocyte RNA by RT-PCR using primers with flanking 5′-BamH-I and 3′-Sal-I sites. The amplicon was cleaved with BamH-I and Sal-I, and ligated to similarly cleaved pLenti.CMV.GFP.puro (658-5; Addgene, Cambridge, MA, USA).[68] To construct pLenti.mtCD40L, the T147N mutation (nt 441 C→A) was introduced into the CD40L cDNA by overlapping PCR. To construct pLenti.CD40L-M1, CD40L was fused to the picornavirus 2A (P2A) sequence[49] and the sequence encoding influenza M1 (GILGFVFTL) by overlapping PCR. The amplicon was cleaved with BamH-I and Sal-I, and ligated to similarly cleaved pLenti.GFP.puro. pLenti.CD40L-SL9 was constructed by overlapping PCR to generate CD40L fused to SL9 (SLYNTVATL) via P2A. To construct pLenti.PD1-CD40L, an amplicon was constructed expressing a codon-optimized PD-1 signal peptide fused to the PD-1 microbody sequence with a 5′ Xba-1 site and a 3′-histidine (8His)-tag and P2A.[23] A second amplicon was generated expressing CD40L with a 5′-P2A and 3′-Sal-I site. The amplicons were fused by overlapping PCR, cleaved with Xba-I and Sal-I, and ligated to pLenti.GFP.puro. pLenti.PD1-mtCD40L was constructed similarly using a mutated CD40L amplicon. To construct pHIV.GFP, pNL4-3.Luc.5R$^-$ was cleaved with Pci-I (nucleotides 6,054 and 7,488) to remove *vpu* and the first 1,269 bp of *env*.[69,70] The fragment was re-ligated with a linker containing an Asc-I site. The resulting plasmid was cleaved with Not-I and Xho-I (nucleotide 8,887), and the amplicon encoding CMV.GFP with flanking 5′-Not-I and 3′-Xho-I sites was inserted, replacing the luciferase gene. To generate pHIV.PD1-CD40L, an amplicon encoding the PD-1 microbody fused to CD40L with flanking 5′-Afe-I and 3′-Xho-I restriction sites was cleaved with Afe-I and Xho-I, and ligated to similarly cleaved pHIV.GFP. HIV.CD40L and HIV.PD1-mtCD40L were constructed similarly using a CD40L or PD1-mtCD40L amplicon. SL9 TCR expression vector pCCL.PPT.hPGK.1.9.IRES.eGFP, pCMV.ΔR8.2.Δvpr, pNFNSX.SL9, pMDL-X, and pcVpx have been previously described.[30,35,71–73] pCDH.mPD-L1 was provided by Adam Mor (NYU School of Medicine). To generate pCDH.mPD-L1, mouse PD-L1 was amplified from PD-L1/B7-H1 (NP_068693) VersaClone cDNA (C0752; R&D, Minneapolis, MN, USA) using primers with flanking 5′-BamH-I and 3′-EcoR-I sites. The amplicon was cleaved with BamH-I and EcoR-I, and ligated to lentiviral vector pCDHblast MCSNard (22662; Addgene).[74]

### Lentiviral Vector Preparation

Lentiviral vector stocks for pLenti plasmids were prepared by cotransfection of 293T cells with lentiviral vector plasmid, pMDL-X,[30] pcVSV-G,[75] pcRev,[75] and pcVpx[30] at a mass ratio of 28:10:7:5:2. Lentiviral vector stocks for NL4-3-based plasmids were prepared by cotransfection of 293T cells with lentiviral vector plasmid, VSV-G, Vpx, and pcRev at a mass ratio of 44:5:4:2. After 48 h, virus-containing supernatant was filtered and pelleted by ultracentrifugation for 1 h through 20% sucrose using a SW 32 Ti rotor at 30,000 rpm. Pelleted virions were resuspended in 1/10 the original volume of RPMI/5% heat-inactivated pooled human serum (GemCell, West Sacramento, CA, USA) and frozen in aliquots at −80°C. Viruses that expressed GFP or CD40L were titered on 293T cells by flow cytometry as the number of GFP$^+$ or CD40L$^+$ cells per milliliter virus. SL9 TCR lentivirus was prepared by cotransfection of 293T cells using the ViraPower Lentiviral Expression System (Invitrogen, Carlsbad, CA, USA) with pCCL.PPT.hPGK.1.9.IRES.eGFP, pCMV.ΔR8.2.Δvpr, and pc-VSV-G as described previously.[72]

To detect HIV-1 Gag in transduced cells, MDDCs ($2 \times 10^5$ cells/well) were plated in 96-well round-bottom dishes and transduced with vectors at MOI = 5. 293T cells ($2 \times 10^5$ cells/well) were plated in a six-well dish and transfected with 4 μg of vector plasmid DNA using Lipofectamine (Invitrogen). Seventy-two hours later, lysates were prepared and analyzed on an immunoblot probed with mouse anti-Gag p24 (Aalto Bio Reagents, Dublin, Ireland) followed by horseradish peroxidase-conjugated goat anti-mouse immunoglobulin G (IgG; Sigma-Aldrich). The membranes were developed and scanned on a LI-COR Biosciences FC Imaging System (LI-COR Biosciences, Lincoln, NE, USA).

### Antibodies and Flow Cytometry

Antibodies for flow cytometry were electron-coupled dye-conjugated anti-CD45 (clone HI30), eFluor 450 or 605NC-conjugated anti-CD3 (clone OKT3), phycoerythrin (PE)-Cy7-conjugated anti-CD4 (clone RPA-T4), Alexa 700 or allophycocyanin (APC) 780-conjugated anti-CD8 (clone SK1), BV510-conjugated anti-CD45RA (clone H100), APC eFluor 780-conjugated anti-CD62L (clone DREG-56), PerCP Cy5.5-conjugated anti-PD-1 (clone ebioJ105), PE-Cy7-conjugated IFNγ (clone 4S.B3) (eBioscience, Waltham, MA, USA), APC-conjugated anti-CD83 (clone HB15), biotin-conjugated anti-ICAM-1 (clone REA266) (Miltenyi, Bergisch Gladbach, Germany), secondary antibody Pacific Orange-conjugated streptavidin (Thermo Fisher Scientific, Waltham, MA, USA), fluorescein isothiocyanate (FITC)-conjugated anti-HLA-DR (clone G46-6), PE-conjugated CD40L (clone 89-76) (BD Biosciences, Franklin Lakes, NJ, USA), PE-conjugated SL9 tetramer (MBL International, Woburn, MA, USA), and BV421-conjucted anti-PD-L1 (clone 10F.9G2; BioLegend, San Diego, CA, USA). To measure intracellular IFNγ, cells were incubated for 6 h in medium containing brefeldin A and analyzed on a LSRII or LSRFortessa (BD Biosciences) using FlowJo software.

### Lentiviral Vector Activation and Maturation of DCs

HSC-DCs were generated as previously described.[50] CD34$^+$ cells were purified from fetal liver on magnetic beads and stored in $1 \times 10^6$ aliquots at −80°C. An aliquot was thawed and expanded for 2–3 weeks in RPMI medium containing 10% fetal bovine serum, 10 ng/mL GM-CSF (Miltenyi), and 5 ng/mL SCF (Miltenyi). To generate

MDDCs, donor leukapheresis products were purchased from the NY Blood Center, and PBMCs were isolated by Ficoll density gradient centrifugation. The monocyte fraction was purified by plastic adherence and differentiated to MDDCs over 4 days in medium supplemented with 110 U/mL GM-CSF (Invitrogen) and 282 U/mL IL-4 (R&D Systems). To assess the effects of lentiviral transduction, HSC-DCs or MDDCs were plated in 96-well round-bottom dishes ($2 \times 10^5$ cells/well) and infected with lentiviral vector at MOI = 2 or treated with LPS (100 ng/mL). Three days later, infectivity was determined by staining the transduced cells with PE-anti-CD40L monoclonal antibody (mAb) and quantifying the number of $GFP^+$ and $CD40L^+$ cells by flow cytometry. To measure maturation, transduced HSC-DCs and MDDCs were stained anti-HLA-DR, anti-CD83, anti-CD86, or anti-ICAM-1 antibodies. To measure activation, supernatant TNF-α, IL-12p70, and IL-6 were measured by cytokine bead array using the Human Inflammatory Cytokine Cytometric Bead Array (BD Biosciences).

### Cell-Based PD-L1 Binding Assays

The clonal 293T cell line 293T.PDL1 that stably expressed PD-L1 was established by transfecting 293T cells with PD-L1 expression vector pCDH.mPD-L1 followed by selection in medium containing 10 μg/mL blasticidin. 293T cells ($2 \times 10^5$ cells/well) in six-well dishes were transduced with lentiviral vector at MOI = 5. At 72 h post-transduction, the culture supernatant was harvested and 100 μL was incubated for 1 h with $1 \times 10^5$ 293T.PDL1 cells in a V-bottom 96-well dish on ice. The cells were washed and stained with BV-421-conjugated anti-PD-L1 antibody and analyzed by flow cytometry. To test PD-1 microbody binding to PD-L1 on bystander MDDCs, MDDCs were labeled with CFSE and cocultured with transduced MDDCs. After 72 h, the cells were stained with anti-PD-L1 antibody and analyzed by flow cytometry.

### Nitriloacetic Acid Pull-Down Assay

To measure supernatant PD-1 microbody, 293T cells ($2 \times 10^5$ cells/well) were plated in six-well dishes and the following day transduced with lentiviral vectors at MOI = 5. At 72 h post-transduction, 0.5 mL of culture supernatant was incubated with 30 μL nickel-nitrilotriacetic acid-agarose beads (QIAGEN, Hilden, Germany) for 1 h in buffer containing 10 mM Tris (pH 8.0), 150 mM NaCl, 2.5% Nonidet P-40 (NP-40). The beads were washed twice, and the bound protein was eluted with Laemmli loading buffer. The proteins were analyzed on an immunoblot probed with mouse anti-His antibody (Invitrogen) and horseradish peroxidase-conjugated goat anti-mouse IgG secondary antibody (Sigma-Aldrich, St. Louis, MO, USA). Proteins were visualized using luminescent substrate and scanned on a LI-COR Biosciences FC Imaging System (LI-COR Biotechnology).

### BLT Mice

Humanized mice were established as described previously.[44,76] In brief, NSG mice were sublethally irradiated and implanted with fetal thymus and liver and $CD34^+$ cells. $CD34^+$ stem cells were purified from fetal liver on anti-CD34 antibody-conjugated magnetic microbeads (Miltenyi). A total of $2–5 \times 10^6$ cells were frozen in $1 \times 10^6$ cell aliquots in Bambanker freezing medium (Bulldog Bio, Portsmouth, NH, USA) for later generation of HSC-DCs. SL9 TCR BLT humanized mice were generated using HLA-A*0201-restricted fetal tissue in which autologous $CD34^+$ cells were plated in retronectin-coated dishes (TaKaRa Bio, Kusatsu, Japan) and transduced with SL9 TCR lentivirus at MOI = 2. Half of the transduced $CD34^+$ cells ($0.25 \times 10^6$) were mixed with 5 μL Matrigel Matrix (Corning, Corning, NY, USA) and implanted under the renal capsule with the fetal thymus tissue. The other half were injected retro-orbitally after transplant.[46] For all humanized mice, the engraftment frequency was determined by staining the blood lymphocytes and splenocytes for human CD45 and found to be 60%–90%, resulting in $0.5–2 \times 10^6$ human lymphocytes/mL in the blood and $1–3 \times 10^7$ human lymphocytes in the spleen. For the SL9 TCR BLT mice, engraftment of the SL9 TCR-transduced $CD34^+$ cells resulted in the expression of SL9 TCR in 0.1%–1.4% of the human CD8 T cells. There was no significant difference in the percentage of SL9 $TCR^+$ CD8 T cells between the different experimental groups. For vaccination of SL9 TCR BLT mice, autologous HSC-DCs ($6.0 \times 10^6$ cells/well) were plated in retronectin-coated six-well dishes and transduced with lentiviral vector at MOI = 2. Ten weeks post-transplantation, the mice were injected with $2 \times 10^6$ untransduced or CD40L-SL9-transduced autologous HSC-DCs. Three weeks post-vaccination, the mice were challenged i.v. with 500 ng NFNSX.SL9, a replication-competent NL4-3 corrected to encode the SL9 epitope.[77] BLT humanized mice with the SL9 TCR were injected with $2 \times 10^6$ transduced autologous HSC-DCs twice over a 2-week period, and 1 week later were challenged with NFNSX.SL9. For all figures except Figures 6B and 6C, data represent a single experiment in which the humanized mice were generated from a single donor. Figures 6B and 6C represent aggregate data from three independent experiments in which the humanized mice were generated from three different donors.

### T Cell Function Assay

Splenocytes from individual mice or from peripheral T cells from a pooled group of mice were incubated with HIV-1 consensus B Gag, Pol, Nef, Rev, and Vif peptide sets (NIH AIDS Reagent Program, Division of AIDS, NIH/NIAID, Germantown, MD, USA). After 16 h, brefeldin A was added for 6 h, and CD8 and $IFN\gamma^+$ expression were analyzed by flow cytometry.

### Plasma Viral Load

Mice were bled by retro-orbital bleeding or heart puncture. The blood was clarified by centrifugation at $350 \times g$, and RNA was purified using a QIAamp Viral RNA Mini Kit (QIAGEN). HIV-1 RNA was quantified by real-time RT-PCR using TaqMan RNA-To-Ct One-Step reagents (Thermo Fisher Scientific) with primers HIV-1_F: 5′-CAATGGCAGCAATTTCACCA-3′ and HIV-1_R: 5′-GAATGC CAAATTCCTGCTTGA-3′ and a probe hybridizing to HIV-1 NL4-3 4603-4626 5′-[6-FAM]CCCACCAACAGGCGGCCTTAA CTG [Tamra-Q]-3′.[40,45]

### Statistics

Statistical significance was determined by Mann-Whitney U tests, Wilcoxon matched-pairs signed rank test, or t tests. Significance

was based on two-sided testing and attributed to $p < 0.05$. Confidence intervals are shown as the mean ± SD or SEM.

### Study Approval

PBMCs were purchased from the NY Blood Center or obtained at UCLA in accordance with University of California, Los Angeles (UCLA) institutional review board (IRB)-approved protocols under written informed consent using an IRB-approved written consent form by the UCLA Center for AIDS Research Virology Laboratory and distributed without personal identifying information. Human fetal tissue was purchased from Advanced Biosciences Resources or obtained from the UCLA Gene and Cellular Tissue Core without identifying information and were exempt from IRB approval. Animal research described here was with the written approval of the UCLA Animal Research Committee in accordance with all federal, state, and local guidelines. All surgeries were performed under ketamine, xylazine, and isoflurane anesthesia, and all efforts were made to minimize animal pain and discomfort.

## SUPPLEMENTAL INFORMATION

Supplemental Information can be found online at https://doi.org/10.1016/j.ymthe.2019.03.008.

## AUTHOR CONTRIBUTIONS

T.D.N. and A.Z. planned the experiments, carried out the experiments, and wrote the manuscript. T.T. and J.K. carried out the experiments and provided intellectual input. S.K. planned the experiments and edited the manuscript. N.R.L. directed the study, planned the experiments, and wrote the manuscript.

## CONFLICTS OF INTEREST

The authors declare no competing interests.

## ACKNOWLEDGMENTS

We thank Sydney Gordon and Aaron Ring for the soluble PD-1 gene, Otto Yang for NFNSX.SL9, and Adam Mor for pCDH.mPD-L1. We thank Valerie Rezek, Noelle Daly, and Brianna Lam for technical assistance with humanized mice. This work was supported by NIH grants AI122390, AI067059, DA046100, AI120898, AI028697, and AI118565, the UCLA Center for AIDS Research, NYU School of Medicine Luis Vargas HIV Research, Saperstein Scholar, Weissmann Scholar, and Chairman's Circle Awards.

## REFERENCES

1. Chun, T.W., Justement, J.S., Murray, D., Hallahan, C.W., Maenza, J., Collier, A.C., Sheth, P.M., Kaul, R., Ostrowski, M., Moir, S., et al. (2010). Rebound of plasma viremia following cessation of antiretroviral therapy despite profoundly low levels of HIV reservoir: implications for eradication. AIDS *24*, 2803–2808.
2. Chun, T.W., Stuyver, L., Mizell, S.B., Ehler, L.A., Mican, J.A., Baseler, M., Lloyd, A.L., Nowak, M.A., and Fauci, A.S. (1997). Presence of an inducible HIV-1 latent reservoir during highly active antiretroviral therapy. Proc. Natl. Acad. Sci. USA *94*, 13193–13197.
3. Finzi, D., Blankson, J., Siliciano, J.D., Margolick, J.B., Chadwick, K., Pierson, T., Smith, K., Lisziewicz, J., Lori, F., Flexner, C., et al. (1999). Latent infection of CD4+ T cells provides a mechanism for lifelong persistence of HIV-1, even in patients on effective combination therapy. Nat. Med. *5*, 512–517.
4. Finzi, D., Hermankova, M., Pierson, T., Carruth, L.M., Buck, C., Chaisson, R.E., Quinn, T.C., Chadwick, K., Margolick, J., Brookmeyer, R., et al. (1997). Identification of a reservoir for HIV-1 in patients on highly active antiretroviral therapy. Science *278*, 1295–1300.
5. Siliciano, J.D., Kajdas, J., Finzi, D., Quinn, T.C., Chadwick, K., Margolick, J.B., Kovacs, C., Gange, S.J., and Siliciano, R.F. (2003). Long-term follow-up studies confirm the stability of the latent reservoir for HIV-1 in resting CD4+ T cells. Nat. Med. *9*, 727–728.
6. Deng, K., Pertea, M., Rongvaux, A., Wang, L., Durand, C.M., Ghiaur, G., Lai, J., McHugh, H.L., Hao, H., Zhang, H., et al. (2015). Broad CTL response is required to clear latent HIV-1 due to dominance of escape mutations. Nature *517*, 381–385.
7. Betts, M.R., Nason, M.C., West, S.M., De Rosa, S.C., Migueles, S.A., Abraham, J., Lederman, M.M., Benito, J.M., Goepfert, P.A., Connors, M., et al. (2006). HIV nonprogressors preferentially maintain highly functional HIV-specific CD8+ T cells. Blood *107*, 4781–4789.
8. Sáez-Cirión, A., Lacabaratz, C., Lambotte, O., Versmisse, P., Urrutia, A., Boufassa, F., Barré-Sinoussi, F., Delfraissy, J.F., Sinet, M., Pancino, G., and Venet, A.; Agence Nationale de Recherches sur le Sida EP36 HIV Controllers Study Group (2007). HIV controllers exhibit potent CD8 T cell capacity to suppress HIV infection ex vivo and peculiar cytotoxic T lymphocyte activation phenotype. Proc. Natl. Acad. Sci. USA *104*, 6776–6781.
9. Yan, J., Sabbaj, S., Bansal, A., Amatya, N., Shacka, J.J., Goepfert, P.A., and Heath, S.L. (2013). HIV-specific CD8+ T cells from elite controllers are primed for survival. J. Virol. *87*, 5170–5181.
10. Khaitan, A., and Unutmaz, D. (2011). Revisiting immune exhaustion during HIV infection. Curr. HIV/AIDS Rep. *8*, 4–11.
11. Wherry, E.J. (2011). T cell exhaustion. Nat. Immunol. *12*, 492–499.
12. Correa-Rocha, R., Lopez-Abente, J., Gutierrez, C., Pérez-Fernández, V.A., Prieto-Sánchez, A., Moreno-Guillen, S., Muñoz-Fernández, M.Á., and Pion, M. (2018). CD72/CD100 and PD-1/PD-L1 markers are increased on T and B cells in HIV-1+ viremic individuals, and CD72/CD100 axis is correlated with T-cell exhaustion. PLoS ONE *13*, e0203419.
13. Day, C.L., Kaufmann, D.E., Kiepiela, P., Brown, J.A., Moodley, E.S., Reddy, S., Mackey, E.W., Miller, J.D., Leslie, A.J., DePierres, C., et al. (2006). PD-1 expression on HIV-specific T cells is associated with T-cell exhaustion and disease progression. Nature *443*, 350–354.
14. Peretz, Y., He, Z., Shi, Y., Yassine-Diab, B., Goulet, J.P., Bordi, R., Filali-Mouhim, A., Loubert, J.B., El-Far, M., Dupuy, F.P., et al. (2012). CD160 and PD-1 co-expression on HIV-specific CD8 T cells defines a subset with advanced dysfunction. PLoS Pathog. *8*, e1002840.
15. Porichis, F., and Kaufmann, D.E. (2012). Role of PD-1 in HIV pathogenesis and as target for therapy. Curr. HIV/AIDS Rep. *9*, 81–90.
16. Borghaei, H., Paz-Ares, L., Horn, L., Spigel, D.R., Steins, M., Ready, N.E., Chow, L.Q., Vokes, E.E., Felip, E., Holgado, E., et al. (2015). Nivolumab versus Docetaxel in Advanced Nonsquamous Non-Small-Cell Lung Cancer. N. Engl. J. Med. *373*, 1627–1639.
17. Brahmer, J., Reckamp, K.L., Baas, P., Crinò, L., Eberhardt, W.E., Poddubskaya, E., Antonia, S., Pluzanski, A., Vokes, E.E., Holgado, E., et al. (2015). Nivolumab versus Docetaxel in Advanced Squamous-Cell Non-Small-Cell Lung Cancer. N. Engl. J. Med. *373*, 123–135.
18. Motzer, R.J., Escudier, B., McDermott, D.F., George, S., Hammers, H.J., Srinivas, S., Tykodi, S.S., Sosman, J.A., Procopio, G., Plimack, E.R., et al.; CheckMate 025 Investigators (2015). Nivolumab versus Everolimus in Advanced Renal-Cell Carcinoma. N. Engl. J. Med. *373*, 1803–1813.
19. Postow, M.A., Chesney, J., Pavlick, A.C., Robert, C., Grossmann, K., McDermott, D., Linette, G.P., Meyer, N., Giguere, J.K., Agarwala, S.S., et al. (2015). Nivolumab and ipilimumab versus ipilimumab in untreated melanoma. N. Engl. J. Med. *372*, 2006–2017.
20. Robert, C., Schachter, J., Long, G.V., Arance, A., Grob, J.J., Mortier, L., Daud, A., Carlino, M.S., McNeil, C., Lotem, M., et al.; KEYNOTE-006 investigators (2015). Pembrolizumab versus Ipilimumab in Advanced Melanoma. N. Engl. J. Med. *372*, 2521–2532.

21. Sharma, P., Retz, M., Siefker-Radtke, A., Baron, A., Necchi, A., Bedke, J., Plimack, E.R., Vaena, D., Grimm, M.O., Bracarda, S., et al. (2017). Nivolumab in metastatic urothelial carcinoma after platinum therapy (CheckMate 275): a multicentre, single-arm, phase 2 trial. Lancet Oncol. *18*, 312–322.

22. Weber, J.S., D'Angelo, S.P., Minor, D., Hodi, F.S., Gutzmer, R., Neyns, B., Hoeller, C., Khushalani, N.I., Miller, W.H., Jr., Lao, C.D., et al. (2015). Nivolumab versus chemotherapy in patients with advanced melanoma who progressed after anti-CTLA-4 treatment (CheckMate 037): a randomised, controlled, open-label, phase 3 trial. Lancet Oncol. *16*, 375–384.

23. Maute, R.L., Gordon, S.R., Mayer, A.T., McCracken, M.N., Natarajan, A., Ring, N.G., Kimura, R., Tsai, J.M., Manglik, A., Kruse, A.C., et al. (2015). Engineering high-affinity PD-1 variants for optimized immunotherapy and immuno-PET imaging. Proc. Natl. Acad. Sci. USA *112*, E6506–E6514.

24. Gay, C.L., Bosch, R.J., Ritz, J., Hataye, J.M., Aga, E., Tressler, R.L., Mason, S.W., Hwang, C.K., Grasela, D.M., Ray, N., et al.; AIDS Clinical Trials 5326 Study Team (2017). Clinical trial of the anti-PD-L1 antibody BMS-936559 in HIV-1 infected participants on suppressive antiretroviral therapy. J. Infect. Dis. *215*, 1725–1733.

25. Coelho, A.V., de Moura, R.R., Kamada, A.J., da Silva, R.C., Guimarães, R.L., Brandão, L.A., de Alencar, L.C., and Crovella, S. (2016). Dendritic Cell-Based Immunotherapies to Fight HIV: How Far from a Success Story? A Systematic Review and Meta-Analysis. Int. J. Mol. Sci. *17*, e1985.

26. García, F., Plana, M., Climent, N., León, A., Gatell, J.M., and Gallart, T. (2013). Dendritic cell based vaccines for HIV infection: the way ahead. Hum. Vaccin. Immunother. *9*, 2445–2452.

27. Palucka, K., and Banchereau, J. (2013). Dendritic-cell-based therapeutic cancer vaccines. Immunity *39*, 38–48.

28. Sabado, R.L., Balan, S., and Bhardwaj, N. (2017). Dendritic cell-based immunotherapy. Cell Res. *27*, 74–95.

29. Norton, T.D., Miller, E.A., Bhardwaj, N., and Landau, N.R. (2015). Vpx-containing dendritic cell vaccine induces CTLs and reactivates latent HIV-1 in vitro. Gene Ther. *22*, 227–236.

30. Sunseri, N., O'Brien, M., Bhardwaj, N., and Landau, N.R. (2011). Human immunodeficiency virus type 1 modified to package Simian immunodeficiency virus Vpx efficiently infects macrophages and dendritic cells. J. Virol. *85*, 6263–6274.

31. Goldstone, D.C., Ennis-Adeniran, V., Hedden, J.J., Groom, H.C., Rice, G.I., Christodoulou, E., Walker, P.A., Kelly, G., Haire, L.F., Yap, M.W., et al. (2011). HIV-1 restriction factor SAMHD1 is a deoxynucleoside triphosphate triphosphohydrolase. Nature *480*, 379–382.

32. Hrecka, K., Hao, C., Gierszewska, M., Swanson, S.K., Kesik-Brodacka, M., Srivastava, S., Florens, L., Washburn, M.P., and Skowronski, J. (2011). Vpx relieves inhibition of HIV-1 infection of macrophages mediated by the SAMHD1 protein. Nature *474*, 658–661.

33. Laguette, N., Sobhian, B., Casartelli, N., Ringeard, M., Chable-Bessia, C., Ségéral, E., Yatim, A., Emiliani, S., Schwartz, O., and Benkirane, M. (2011). SAMHD1 is the dendritic- and myeloid-cell-specific HIV-1 restriction factor counteracted by Vpx. Nature *474*, 654–657.

34. Lahouassa, H., Daddacha, W., Hofmann, H., Ayinde, D., Logue, E.C., Dragin, L., Bloch, N., Maudet, C., Bertrand, M., Gramberg, T., et al. (2012). SAMHD1 restricts the replication of human immunodeficiency virus type 1 by depleting the intracellular pool of deoxynucleoside triphosphates. Nat. Immunol. *13*, 223–228.

35. Bobadilla, S., Sunseri, N., and Landau, N.R. (2013). Efficient transduction of myeloid cells by an HIV-1-derived lentiviral vector that packages the Vpx accessory protein. Gene Ther. *20*, 514–520.

36. van Kooten, C., and Banchereau, J. (2000). CD40-CD40 ligand. J. Leukoc. Biol. *67*, 2–17.

37. Kim, Y., Anderson, J.L., and Lewin, S.R. (2018). Getting the "Kill" into "Shock and Kill": Strategies to Eliminate Latent HIV. Cell Host Microbe *23*, 14–26.

38. Margolis, D.M., and Archin, N.M. (2017). Proviral Latency, Persistent Human Immunodeficiency Virus Infection, and the Development of Latency Reversing Agents. J. Infect. Dis. *215* (*Suppl 3*), S111–S118.

39. Marsden, M.D., and Zack, J.A. (2017). Humanized Mouse Models for Human Immunodeficiency Virus Infection. Annu. Rev. Virol. *4*, 393–412.

40. Zhen, A., Rezek, V., Youn, C., Lam, B., Chang, N., Rick, J., Carrillo, M., Martin, H., Kasparian, S., Syed, P., et al. (2017). Targeting type I interferon-mediated activation restores immune function in chronic HIV infection. J. Clin. Invest. *127*, 260–268.

41. Karpel, M.E., Boutwell, C.L., and Allen, T.M. (2015). BLT humanized mice as a small animal model of HIV infection. Curr. Opin. Virol. *13*, 75–80.

42. Dudek, T.E., and Allen, T.M. (2013). HIV-specific $CD8^+$ T-cell immunity in humanized bone marrow-liver-thymus mice. J. Infect. Dis. *208* (*Suppl 2*), S150–S154.

43. Dudek, T.E., No, D.C., Seung, E., Vrbanac, V.D., Fadda, L., Bhoumik, P., Boutwell, C.L., Power, K.A., Gladden, A.D., Battis, L., et al. (2012). Rapid evolution of HIV-1 to functional $CD8^+$ T cell responses in humanized BLT mice. Sci. Transl. Med. *4*, 143ra98.

44. Kitchen, S.G., Levin, B.R., Bristol, G., Rezek, V., Kim, S., Aguilera-Sandoval, C., Balamurugan, A., Yang, O.O., and Zack, J.A. (2012). In vivo suppression of HIV by antigen specific T cells derived from engineered hematopoietic stem cells. PLoS Pathog. *8*, e1002649.

45. Zhen, A., Kamata, M., Rezek, V., Rick, J., Levin, B., Kasparian, S., Chen, I.S., Yang, O.O., Zack, J.A., and Kitchen, S.G. (2015). HIV-specific Immunity Derived From Chimeric Antigen Receptor-engineered Stem Cells. Mol. Ther. *23*, 1358–1367.

46. Zhen, A., Rezek, V., Youn, C., Rick, J., Lam, B., Chang, N., Zack, J., Kamata, M., and Kitchen, S. (2016). Stem-cell Based Engineered Immunity Against HIV Infection in the Humanized Mouse Model. J. Vis. Exp. *113*, e54048.

47. Seyama, K., Nonoyama, S., Gangsaas, I., Hollenbaugh, D., Pabst, H.F., Aruffo, A., and Ochs, H.D. (1998). Mutations of the CD40 ligand gene and its effect on CD40 ligand expression in patients with X-linked hyper IgM syndrome. Blood *92*, 2421–2434.

48. Bednarek, M.A., Sauma, S.Y., Gammon, M.C., Porter, G., Tamhankar, S., Williamson, A.R., and Zweerink, H.J. (1991). The minimum peptide epitope from the influenza virus matrix protein. Extra and intracellular loading of HLA-A2. J. Immunol. *147*, 4047–4053.

49. Szymczak, A.L., Workman, C.J., Wang, Y., Vignali, K.M., Dilioglou, S., Vanin, E.F., and Vignali, D.A. (2004). Correction of multi-gene deficiency in vivo using a single 'self-cleaving' 2A peptide-based retroviral vector. Nat. Biotechnol. *22*, 589–594.

50. Harada, Y., Okada-Nakanishi, Y., Ueda, Y., Tsujitani, S., Saito, S., Fuji-Ogawa, T., Iida, A., Hasegawa, M., Ichikawa, T., and Yonemitsu, Y. (2011). Cytokine-based high log-scale expansion of functional human dendritic cells from cord-blood CD34-positive cells. Sci. Rep. *1*, 174.

51. Barber, D.L., Wherry, E.J., Masopust, D., Zhu, B., Allison, J.P., Sharpe, A.H., Freeman, G.J., and Ahmed, R. (2006). Restoring function in exhausted CD8 T cells during chronic viral infection. Nature *439*, 682–687.

52. Ahmed, Z., Kawamura, T., Shimada, S., and Piguet, V. (2015). The role of human dendritic cells in HIV-1 infection. J. Invest. Dermatol. *135*, 1225–1233.

53. Miller, E., and Bhardwaj, N. (2013). Dendritic cell dysregulation during HIV-1 infection. Immunol. Rev. *254*, 170–189.

54. Wu, L., and KewalRamani, V.N. (2006). Dendritic-cell interactions with HIV: infection and viral dissemination. Nat. Rev. Immunol. *6*, 859–868.

55. Collins, K.L., Chen, B.K., Kalams, S.A., Walker, B.D., and Baltimore, D. (1998). HIV-1 Nef protein protects infected primary cells against killing by cytotoxic T lymphocytes. Nature *391*, 397–401.

56. Schwartz, O., Maréchal, V., Le Gall, S., Lemonnier, F., and Heard, J.M. (1996). Endocytosis of major histocompatibility complex class I molecules is induced by the HIV-1 Nef protein. Nat. Med. *2*, 338–342.

57. Cunningham, C.R., Champhekar, A., Tullius, M.V., Dillon, B.J., Zhen, A., de la Fuente, J.R., Herskovitz, J., Elsaesser, H., Snell, L.M., Wilson, E.B., et al. (2016). Type I and Type II Interferon Coordinately Regulate Suppressive Dendritic Cell Fate and Function during Viral Persistence. PLoS Pathog. *12*, e1005356.

58. Sperk, M., Domselaar, R.V., and Neogi, U. (2018). Immune Checkpoints as the Immune System Regulators and Potential Biomarkers in HIV-1 Infection. Int. J. Mol. Sci. *19*, e2000.

59. Trautmann, L., Janbazian, L., Chomont, N., Said, E.A., Gimmig, S., Bessette, B., Boulassel, M.R., Delwart, E., Sepulveda, H., Balderas, R.S., et al. (2006). Upregulation of PD-1 expression on HIV-specific CD8+ T cells leads to reversible immune dysfunction. Nat. Med. *12*, 1198–1202.

60. Pardoll, D.M. (2012). The blockade of immune checkpoints in cancer immunotherapy. Nat. Rev. Cancer *12*, 252–264.

61. Seung, E., Dudek, T.E., Allen, T.M., Freeman, G.J., Luster, A.D., and Tager, A.M. (2013). PD-1 blockade in chronically HIV-1-infected humanized mice suppresses viral loads. PLoS ONE *8*, e77780.

62. Hui, E., Cheung, J., Zhu, J., Su, X., Taylor, M.J., Wallweber, H.A., Sasmal, D.K., Huang, J., Kim, J.M., Mellman, I., and Vale, R.D. (2017). T cell costimulatory receptor CD28 is a primary target for PD-1-mediated inhibition. Science *355*, 1428–1433.

63. Ahn, E., Araki, K., Hashimoto, M., Li, W., Riley, J.L., Cheung, J., Sharpe, A.H., Freeman, G.J., Irving, B.A., and Ahmed, R. (2018). Role of PD-1 during effector CD8 T cell differentiation. Proc. Natl. Acad. Sci. USA *115*, 4749–4754.

64. Marsden, M.D., Loy, B.A., Wu, X., Ramirez, C.M., Schrier, A.J., Murray, D., Shimizu, A., Ryckbosch, S.M., Near, K.E., Chun, T.W., et al. (2017). In vivo activation of latent HIV with a synthetic bryostatin analog effects both latent cell "kick" and "kill" in strategy for virus eradication. PLoS Pathog. *13*, e1006575.

65. Shan, L., Deng, K., Shroff, N.S., Durand, C.M., Rabi, S.A., Yang, H.C., Zhang, H., Margolick, J.B., Blankson, J.N., and Siliciano, R.F. (2012). Stimulation of HIV-1-specific cytolytic T lymphocytes facilitates elimination of latent viral reservoir after virus reactivation. Immunity *36*, 491–501.

66. Figdor, C.G., de Vries, I.J., Lesterhuis, W.J., and Melief, C.J. (2004). Dendritic cell immunotherapy: mapping the way. Nat. Med. *10*, 475–480.

67. Naidoo, J., Page, D.B., Li, B.T., Connell, L.C., Schindler, K., Lacouture, M.E., Postow, M.A., and Wolchok, J.D. (2015). Toxicities of the anti-PD-1 and anti-PD-L1 immune checkpoint antibodies. Ann. Oncol. *26*, 2375–2391.

68. Campeau, E., Ruhl, V.E., Rodier, F., Smith, C.L., Rahmberg, B.L., Fuss, J.O., Campisi, J., Yaswen, P., Cooper, P.K., and Kaufman, P.D. (2009). A versatile viral system for expression and depletion of proteins in mammalian cells. PLoS ONE *4*, e6529.

69. Connor, R.I., Chen, B.K., Choe, S., and Landau, N.R. (1995). Vpr is required for efficient replication of human immunodeficiency virus type-1 in mononuclear phagocytes. Virology *206*, 935–944.

70. He, J., Choe, S., Walker, R., Di Marzio, P., Morgan, D.O., and Landau, N.R. (1995). Human immunodeficiency virus type 1 viral protein R (Vpr) arrests cells in the G2 phase of the cell cycle by inhibiting p34cdc2 activity. J. Virol. *69*, 6705–6711.

71. Bennett, M.S., Joseph, A., Ng, H.L., Goldstein, H., and Yang, O.O. (2010). Fine-tuning of T-cell receptor avidity to increase HIV epitope variant recognition by cytotoxic T lymphocytes. AIDS *24*, 2619–2628.

72. Kitchen, S.G., Bennett, M., Galić, Z., Kim, J., Xu, Q., Young, A., Lieberman, A., Joseph, A., Goldstein, H., Ng, H., et al. (2009). Engineering antigen-specific T cells from genetically modified human hematopoietic stem cells in immunodeficient mice. PLoS ONE *4*, e8208.

73. Poon, B., Hsu, J.F., Gudeman, V., Chen, I.S., and Grovit-Ferbas, K. (2005). Formaldehyde-treated, heat-inactivated virions with increased human immunodeficiency virus type 1 env can be used to induce high-titer neutralizing antibody responses. J. Virol. *79*, 10210–10217.

74. Pegoraro, G., Kubben, N., Wickert, U., Göhler, H., Hoffmann, K., and Misteli, T. (2009). Ageing-related chromatin defects through loss of the NURD complex. Nat. Cell Biol. *11*, 1261–1267.

75. Dull, T., Zufferey, R., Kelly, M., Mandel, R.J., Nguyen, M., Trono, D., and Naldini, L. (1998). A third-generation lentivirus vector with a conditional packaging system. J. Virol. *72*, 8463–8471.

76. Marsden, M.D., Kovochich, M., Suree, N., Shimizu, S., Mehta, R., Cortado, R., Bristol, G., An, D.S., and Zack, J.A. (2012). HIV latency in the humanized BLT mouse. J. Virol. *86*, 339–347.

77. Shimizu, S., Hong, P., Arumugam, B., Pokomo, L., Boyer, J., Koizumi, N., Kittipongdaja, P., Chen, A., Bristol, G., Galic, Z., et al. (2010). A highly efficient short hairpin RNA potently down-regulates CCR5 expression in systemic lymphoid organs in the hu-BLT mouse model. Blood *115*, 1534–1544.

YMTHE, Volume *27*

## Supplemental Information

# Lentiviral Vector-Based Dendritic Cell Vaccine Suppresses HIV Replication in Humanized Mice

**Thomas D. Norton, Anjie Zhen, Takuya Tada, Jennifer Kim, Scott Kitchen, and Nathaniel R. Landau**

**Supplementary Materials**

**Supplementary Methods**

**Viral RNA sequence analysis for escape mutants**

Plasma and PBMC RNA prepared from HIV-1-infected BLT mice were reverse transcribed to generate cDNA from which amplicons spanning NL4-3 *gag* (bp 931-1111) in the region encoding SL9 were generated by nested PCR using the following primer pairs: outer primers: TGGGTGCGAGAGCGTCGGTAT and TCTATCCCATTCTGCAGCTTCCTC, inner primers: CCTGGCCTTTTAGAGACATCAG and GCTCTTCCTCTATCTTATCTAAGGC. Amplified DNA fragments were cloned using TOPO TA cloning (Invitrogen) and sequenced.

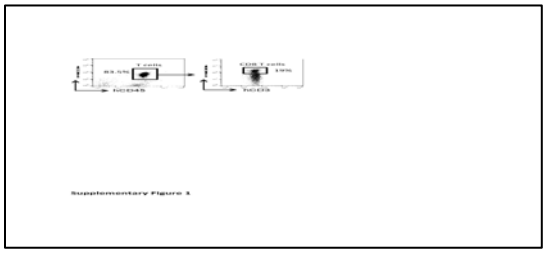

**Figure S1**. **BLT mice express high-levels of human T cells**. The gating strategy used to analyze human CD8 T cells from the peripheral blood of BLT humanized mice based on the expression of human CD45, CD3 and CD8 is shown.

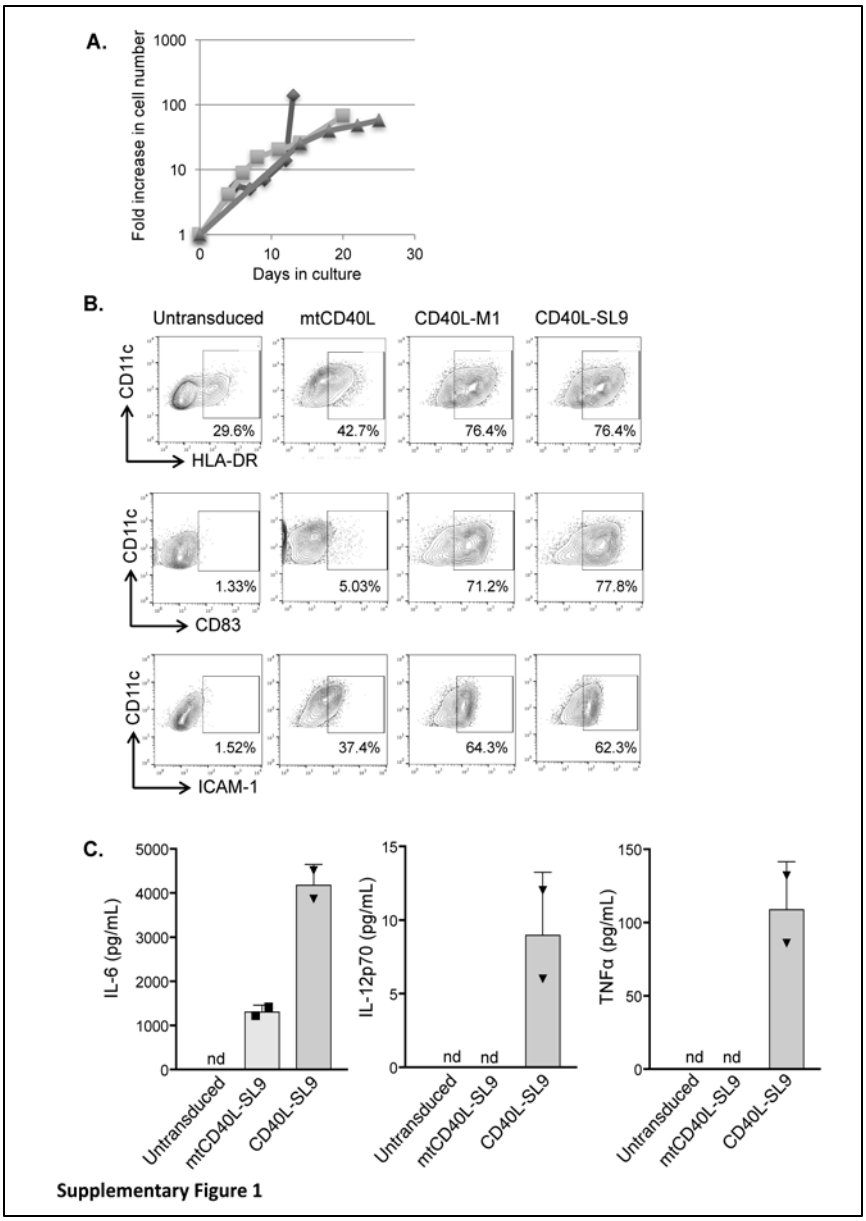


**Figure S2**. **HSCs treated with GM-CSF and SCF expand in log-scale to generate human DCs that mature in response to transduction with CD40L-expressing vectors**. (**A**) Fetal liver-derived HSCs were cultured for three weeks with GM-CSF and SCF to generate HSC-DCs. Shown are the number of cells in culture plotted as fold increase over time. (**B**) HSC-DCs were transduced with mtCD40L, CD40L-M1 or CD40L-SL9 vectors and after 72 h the percentage of HLA-DR+, CD83+ and ICAM-1+ cells was quantified by flow cytometry. Experiments were done in three donors. Representative blots from one donor are shown. (**C**) IL-6, IL-12p70, and TNFα in the transduced HSC-DC supernatant were quantified by cytokine bead array. Data represent mean ± SD from one donor analyzed in two independent experiments. nd = not detected.

Plasma RNA

| Vaccination | Mice | Clones | WT SL9 epitopes (%) | Mutated SL9 epitopes (%) |
|---|---|---|---|---|
| No HSC-DCs | 4 | 19 | 18/19 (95%) | SLYNTVA**A**L 1/19 (5%) |
| Untransduced HSC-DCs | 3 | 13 | 8/13 (61%) | SLYNT**I**A**V**L 4/13 (31%)<br>SLYNTVAT**P** 1/13 (8%) |
| CD40L-SL9 HSC-DCs | 4 | 20 | 18/20 (90%) | **P**LYNTVATL 2/20 (10%) |


PBMC cellular RNA

| Vaccination | Mice | Clones | WT SL9 epitopes (%) | Mutated SL9 epitopes (%) |
|---|---|---|---|---|
| No HSC-DCs | 5 | 22 | 20/22 (91%) | SLYNTVAT**F** 1/22 (4.5%)<br>**T**LYNTVATL 1/22 (4.5%) |
| Untransduced HSC-DCs | 2 | 9 | 8/9 (89%) | SLYNT**I**A**V**L 1/9 (11%) |
| CD40L-SL9 HSC-DCs | 4 | 18 | 17/18 (94%) | SLYNT**I**A**V**L 1/18 (6%) |


**Supplementary Figure 3**

**Figure S3**. **Virus rebound is not driven by SL9 escape mutations**. Plasma RNA and PBMC cellular RNA from unvaccinated and HSC-DC vaccinated humanized mice were reverse transcribed to generate cDNA from which amplicons spanning the HIV-1 Gag region encoding the SL9 epitope were generated by nested PCR and cloned by TOPA TA cloning. Up to five clones per mouse were sequenced and the number of WT and mutant SL9 epitopes and corresponding pie charts for plasma RNA (top) and cellular RNA (bottom) isolates are shown.

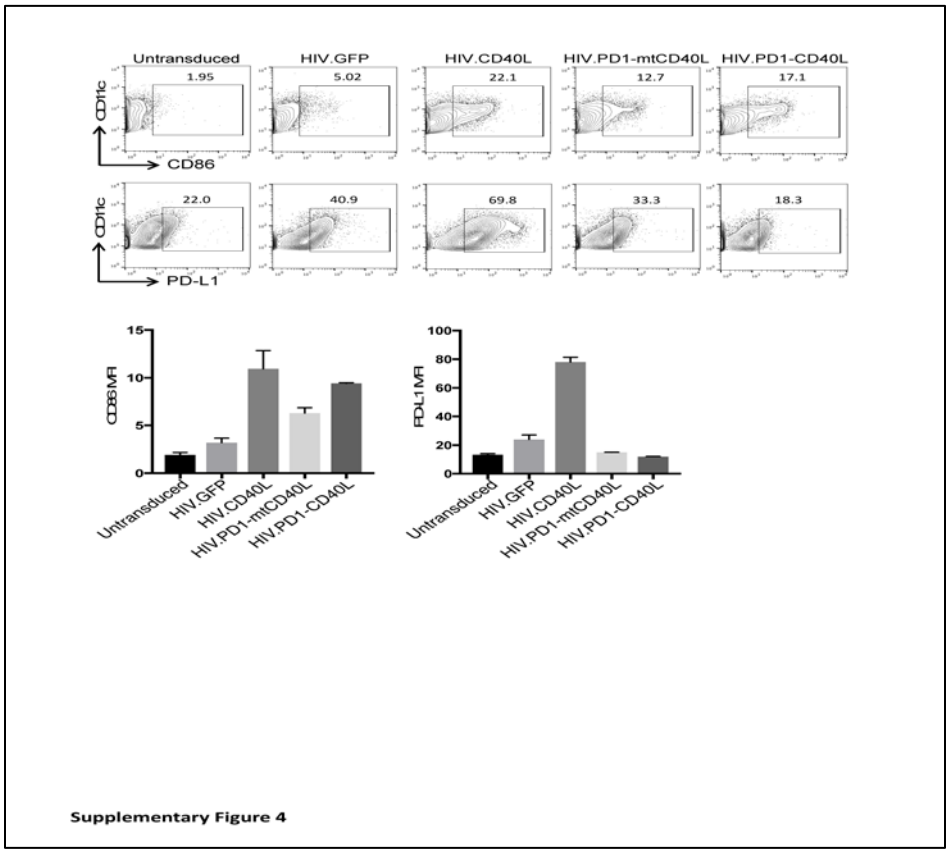


**Figure S4**. **Co-expression of CD40L and PD-1 microbody enhances HSC-DC maturation while masking PD-L1**. HSC-DCs were untransduced or transduced with HIV.GFP, HIV.CD40L, HIV.PD1-mtCD40L or HIV.PD1-CD40L vectors and 72 h later the frequency of CD86+ or PD-L1+ CD11c+ cells was measured by flow cytometry. Representative blots are shown (top). Pooled data showing the CD86 and PD-L1 MFIs of CD11c+ cells derived from two different aliquots of donor CD34+ HSCs that were separately differentiated to HSC-DCs and transduced with the lentiviral vectors are shown (bottom). Data represent mean ± SEM.

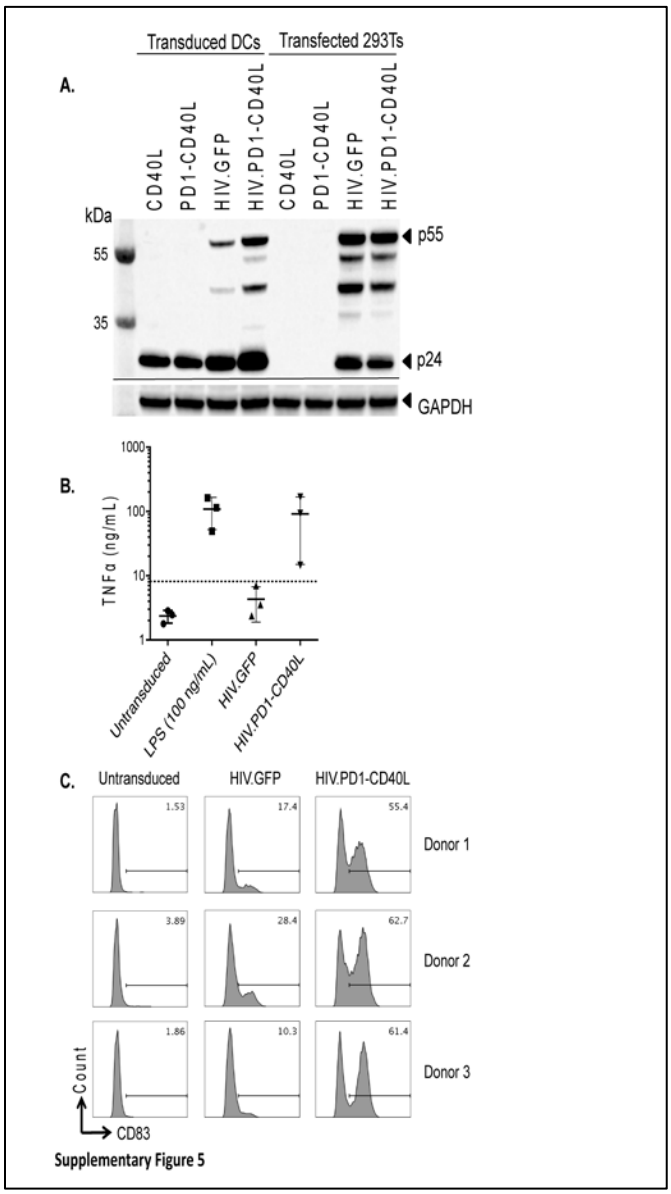


**Figure S5**. **HIV.PD1-CD40L-transduced MDDCs express HIV proteins and mature and become activated**. (**A**) Donor MDDCs were transduced with CD40L, PD1-CD40L, HIV.GFP or HIV.PD1-CD40L vectors (left) or transfected with the corresponding plasmids (right). At 72 h post-transduction or post-transfection, Gag protein and GAPDH in the cell lysates was detected by western blot. (**B**) MDDCs were transduced with HIV.GFP or HIV.PD1-CD40L vectors. Untransduced and LPS-treated MDDCs served as controls. After 72 h, supernatant TNFα was quantified by cytokine bead array and flow cytometry. Pooled results from three donors are shown. Data represent mean ± SD. The dotted line indicates the limit of detection. (**C**) MDDC expression of the maturation marker CD83 is shown for each donor.